Behavioral/Systems/Cognitive

Serotonin 5-HT$_{1A}$ Receptors Regulate NMDA Receptor Channels through a Microtubule-Dependent Mechanism

Eunice Y. Yuen, Qian Jiang, Paul Chen, Zhenglin Gu, Jian Feng, and Zhen Yan
Department of Physiology and Biophysics, School of Medicine and Biomedical Sciences, State University of New York at Buffalo, Buffalo, New York 14214

The serotonin system and NMDA receptors (NMDARs) in prefrontal cortex (PFC) are both critically involved in the regulation of cognition and emotion under normal and pathological conditions; however, the interactions between them are essentially unknown. Here we show that serotonin, by activating 5-HT$_{1A}$ receptors, inhibited NMDA receptor-mediated ionic and synaptic currents in PFC pyramidal neurons, and the NR2B subunit-containing NMDA receptor is the primary target of 5-HT$_{1A}$ receptors. This effect of 5-HT$_{1A}$ receptors was blocked by agents that interfere with microtubule assembly, as well as by cellular knock-down of the kinesin motor protein KIF17 (kinesin superfamily member 17), which transports NR2B-containing vesicles along microtubule in neuronal dendrites. Inhibition of either CaMKII (calcium/calmodulin-dependent kinase II) or MEK/ERK (mitogen-activated protein kinase kinase/extracellular signal-regulated kinase) abolished the 5-HT$_{1A}$ modulation of NMDAR currents. Biochemical evidence also indicates that 5-HT$_{1A}$ activation reduced microtubule stability, which was abolished by CaMKII or MEK inhibitors. Moreover, immunocytochemical studies show that 5-HT$_{1A}$ activation decreased the number of surface NR2B subunits on dendrites, which was prevented by the microtubule stabilizer. Together, these results suggest that serotonin suppresses NMDAR function through a mechanism dependent on microtubule/kinesin-based dendritic transport of NMDA receptors that is regulated by CaMKII and ERK signaling pathways. The 5-HT$_{1A}$–NMDAR interaction provides a potential mechanism underlying the role of serotonin in controlling emotional and cognitive processes subserved by PFC.

Key words: **trafficking; KIF17; MAP2; Ca^{2+}/calmodulin-dependent kinase II; MAP kinase; prefrontal cortex; siRNA; antisense oligonucleotides**

Introduction

The serotonergic system in prefrontal cortex (PFC) plays a critical role in controlling emotion and cognition under normal and pathological conditions (Dubovsky and Thomas 1995; Buhot, 1997; Davidson et al., 2000). The pleiotropic functions of serotonin are afforded by the concerted actions of multiple serotonin receptor subtypes (Andrade, 1998; Martin et al., 1998). Among them, 5-HT$_{1A}$ receptors are highly enriched in prefrontal cortex (Kia et al., 1996a; Feng et al., 2001). Increased prefrontal 5-HT$_{1A}$ receptor density has been found in schizophrenia patients (Simpson et al., 1996; Sumiyoshi et al., 1996). Mice lacking 5-HT$_{1A}$ receptors show elevated anxiety (Heisler et al., 1998; Ramboz et al., 1998), and this defect can be rescued by expression of 5-HT$_{1A}$ receptors in the forebrain (Gross et al., 2002). A single nucleotide polymorphism in the 5-HT$_{1A}$ receptor promoter has been associated with both anxiety- and depression-related traits in humans (Lemonde et al., 2003; Strobel et al., 2003). Moreover, activation of 5-HT$_{1A}$ receptors has detrimental effects on working memory, and 5-HT$_{1A}$ antagonists ameliorate the cognitive impairment (Carli et al., 1995). Thus, growing attention has been directed toward developing pharmacological agents that target 5-HT$_{1A}$ receptors for the treatment of schizophrenia, anxiety, depression, and cognitive disorders (Schreiber and De Vry, 1993; Meltzer 1999; Bantick et al., 2001; Gross and Hen, 2004).

Because 5-HT$_{1A}$ receptors play a critical role in a variety of mental diseases, it is essential to understand the targets of 5-HT$_{1A}$ receptors that are important for emotion and cognition. Postsynaptic 5-HT$_{1A}$ receptors are found only in the dendritic compartment and associated with dendritic spines (Kia et al., 1996b) in which glutamate receptors are concentrated, raising the possibility that 5-HT$_{1A}$ receptors may exert some of their functions by modulating glutamatergic signaling. The NMDA glutamate receptor, a principal subtype of excitatory ligand-gated ion channel, has been implicated in multiple neuronal functions ranging from synapse formation to synaptic plasticity to learning and memory (Dingledine et al., 1999). Systemic administration of noncompetitive NMDA receptor (NMDAR) antagonists or knock-down the expression of NMDA receptors produces schizophrenia-like behavioral symptoms (Jentsch and Roth, 1999; Mohn et al., 1999); hence, dysfunction of NMDA receptors is strongly linked to the pathophysiology of mental disorders (Tsai and Coyle, 2002). It prompts us to hypothesize that one important target of 5-HT$_{1A}$ receptors could be the NMDA receptor, and dysregulation of glutamatergic transmission and plasticity by altered serotonin system may contribute to the progress of neuropsychiatric disorders.

Received Nov. 18, 2004; revised April 30, 2005; accepted May 1, 2005.

This work was supported by National Institutes of Health Grants MH63128, NS48911, and AG21923, National Science Foundation Grant IBN-0117026, and a National Alliance for Research on Schizophrenia and Depression Independent Investigator Award (Z.Y.). We thank Xiaoqing Chen and Dr. Wade Sigurdson for their technical support. We are grateful to Dr. S. Vicini for kindly providing us with the GFP-tagged NR2B construct.

Correspondence should be addressed to Dr. Zhen Yan, Department of Physiology and Biophysics, State University of New York at Buffalo, 124 Sherman Hall, Buffalo, NY 14214. E-mail: zhenyan@buffalo.edu.

DOI:10.1523/JNEUROSCI.1187-05.2005

 0270-6474/05/255488-14$15.00/0

In this study, we examined the serotonergic regulation of NMDA receptors in PFC pyramidal neurons. We found that serotonin, by activating 5-HT_{1A} receptors, inhibits NMDAR currents through a mechanism dependent on the motor protein-mediated transport of NMDA receptors along microtubules in dendrites. Inhibition of either CaMKII (calcium/calmodulin-dependent kinase II) or ERKs (extracellular signal-regulated kinases), both of which regulate microtubule dynamics, prevents the serotonergic regulation of NMDA receptors. Given the critical role of NMDA signaling in controlling synaptic plasticity and neuronal activity, our results provide a potential molecular and cellular mechanism for 5-HT_{1A} regulation of emotion and cognition in PFC circuits.

Materials and Methods

Acute-dissociation procedure. PFC neurons from young adult (3–4 weeks postnatal) rats were acutely dissociated using procedures similar to those described previously (Feng et al., 2001; Chen et al., 2004). All experiments were performed with the approval of State University of New York at Buffalo Animal Care Committee. After incubation of brain slices in $NaHCO_3$-buffered saline, PFC was dissected and placed in an oxygenated chamber containing papain (0.8 mg/ml; Sigma, St. Louis, MO) in HEPES-buffered HBSS (Sigma) at room temperature. After 40 min of enzyme digestion, tissue was rinsed three times in the low Ca^{2+}, HEPES-buffered saline and mechanically dissociated with a graded series of fire-polished Pasteur pipettes. The cell suspension was then plated into a 35 mm Lux Petri dish, which was then placed on the stage of a Nikon (Tokyo, Japan) inverted microscope.

Primary neuronal culture. Rat PFC cultures were prepared by modification of previously described methods (Wang et al., 2003). Briefly, PFC was dissected from 18 d rat embryos, and cells were dissociated using trypsin and trituration through a Pasteur pipette. The neurons were plated on coverslips coated with poly-L-lysine in DMEM with 10% fetal calf serum at a density of 3000 cells/cm^2. When neurons attached to the coverslip within 24 h, the medium was changed to Neurobasal with B27 supplement. Neurons were maintained for 3 weeks before being used for recordings.

Whole-cell recordings. Pyramidal neurons located in the intermediate and deep layers (III–VI) of the rat PFC were recorded. Recordings of whole-cell ion channel currents used standard voltage-clamp techniques (Yan et al., 1999; Wang et al., 2003; Tyszkiewicz et al., 2004). The internal solution consisted of the following (in mM): 180 *N*-methyl-D-glucamine, 40 HEPES, 4 $MgCl_2$, 0.1 BAPTA, 12 phosphocreatine, 3 Na_2ATP, 0.5 Na_2GTP, and 0.1 leupeptin, pH 7.2–7.3 (265–270 mOsm/l). The external solution consisted of the following (in mM): 127 NaCl, 20 CsCl, 10 HEPES, 1 $CaCl_2$, 5 $BaCl_2$, 12 glucose, 0.001 TTX, and 0.02 glycine, pH 7.3–7.4 (300–305 mOsm/l). Recordings were obtained with an Axon Instruments (Union City, CA) 200B patch-clamp amplifier that was controlled and monitored with an IBM personal computer running pClamp (version 8) with a DigiData 1320 series interface (Axon Instruments). Electrode resistances were typically 2–4 MΩ in the bath. After seal rupture, series resistance (4–10 MΩ) was compensated (70–90%) and periodically monitored. The cell membrane potential was held at −60 mV. The application of NMDA (100 μM) evoked a partially desensitizing inward current that could be blocked by the NMDA receptor antagonist D-APV (50 μM). NMDA was applied alone for 2 s every 30 s to minimize desensitization-induced decrease of current amplitude. Drugs were applied with a gravity-fed "sewer pipe" system. The array of application capillaries (~150 μm inner diameter) was positioned a few hundred micrometers from the cell under study. Solution changes were affected by the SF-77B fast-step solution stimulus delivery device (Warner Instruments, Hamden, CT).

For the recording of miniature EPSCs (mEPSCs) in PFC cultures, the internal solution consisted of the following (in mM): 130 Cs-methanesulfonate, 10 CsCl, 4 NaCl, 10 HEPES, 1 $MgCl_2$, 5 EGTA, 2.2 *N*-ethyl bromide quaternary salt (QX-314), 12 phosphocreatine, 5 MgATP, 0.5 Na_2GTP, and 0.1 leupeptin, pH 7.2–7.3 (265–270 mOsm/l). To record both NMDAR and AMPAR-mediated components of mEPSCs, the external solution consisted of the following (in mM): 127 NaCl, 5 KCl, 2 $CaCl_2$, 12 glucose, 10 HEPES, 0.001 TTX, 0.005 bicuculline, and 0.02 glycine, pH 7.3–7.4 (300–305 mOsm/l). Then the neuron under recording was switched to the external solution with Mg^{2+} (2 mM) and D-APV (20 μM) added to record the AMPAR-mediated component of mEPSCs. After subtracting the AMPAR-mediated component of mEPSCs (averaged trace) from the total mEPSCs(averaged trace), the NMDAR-mediated component of mEPSCs (averaged trace) was revealed. The NMDAR mEPSCs in the absence or presence of agonists were compared.

Serotonin receptor ligands 8-hydroxy-2(di-*n*-propylamino)tetralin (8-OH-DPAT), 5-HT, 1-(2-methoxyphenyl)-4-[4-(2-phthalimido)butyl] piperazine (NAN-190), *N*-[2-[4-(2-methoxyphenyl)-1-piperazinyl]ethyl]-*N*-(2-pyridinyl)cyclohexane-carboxamide (WAY-100635), methysergide, and α-Me-5-HT, the microtubule agents nocodazole, colchicines, and taxol (Sigma), as well as the second-messenger reagents KN-93, KN-92, autocamtide-2-related inhibitory peptide (AIP), calmodulin, calmidazolium (CDZ) and myosin light chain kinase peptide (MLCKP), 2-(2-amino-3-methoxyphenyl)-4*H*-1-benzopyran-4-one (PD98059), 1,4-diamino-2,3-dicyano-1,4-bis(2-aminophynyltio)butadiene (U0126), cpt-cAMP, myristoylated PKI_{14-22} (PKA inhibitory peptide), PKI[5–24], okadaic acid (OA), 1-[6[[(17β)-3-methoxyestra-1,3,5(10)-trien-17-yl]amino]hexyl]-1*H*-pyrrole-2,5-dione (U73122), 2-aminoethoxydiphenylborane (2APB), and calphostin C (Calbiochem, La Jolla, CA) were made up as concentrated stocks in water or DMSO and stored at −20°C. Stocks were thawed and diluted immediately before use. The amino acid sequence for the dynamin inhibitory peptide is QVPSRPNRAP. The amino acid sequence for the phosphorylated inhibitor-1 (I-1) peptide p^{Thr35}I-1[7–39] is PRKIQFTVPLLEPHLDPEAAEQIRRRRP(pT)PATL.

Data analyses were performed with AxoGraph (Axon Instruments), Kaleidagraph (Albeck Software, Reading, PA), Origin 6 (Microcal Software, Northampton, MA), and Statview (Abacus Concepts, Calabasas, CA). For analysis of statistical significance, Mann–Whitney *U* tests were performed to compare the current amplitudes in the presence or absence of agonists. ANOVA tests were performed to compare the differential degrees of current modulation between groups subjected to different treatment.

Electrophysiological recordings in slices. To evaluate the regulation of NMDAR-mediated EPSCs by 5-HT_{1A} receptors in PFC slices, the whole-cell voltage-clamp recording technique was used (Wang et al., 2003; Zhong et al., 2003). Electrodes (5–9 MΩ) were filled with the following internal solution (in mM): 130 Cs-methanesulfonate, 10 CsCl, 4 NaCl, 10 HEPES, 1 $MgCl_2$, 5 EGTA, 2.2 QX-314, 12 phosphocreatine, 5 MgATP, 0.2 Na_3GTP, and 0.1 leupeptin, pH 7.2–7.3 (265–270 mOsm/l). The slice (300 μm) was placed in a perfusion chamber attached to the fixed stage of an upright microscope (Olympus Optical, Tokyo, Japan) and submerged in continuously flowing oxygenated artificial CSF (ACSF). Cells were visualized with a 40× water-immersion lens and illuminated with near infrared (IR) light, and the image was detected with an IR-sensitive CCD camera. A Multiclamp 700A amplifier was used for these recordings. Tight seals (2–10 GΩ) from visualized pyramidal neurons were obtained by applying negative pressure. The membrane was disrupted with additional suction, and the whole-cell configuration was obtained. The access resistances ranged from 13 to 18 MΩ and were compensated 50–70%. For the recording of NMDAR-mediated evoked EPSCs, cells were bathed in ACSF containing CNQX (20 μM) and bicuculline (10 μM) to block AMPA/kainate receptors and $GABA_A$ receptors. Evoked currents were generated with a 50 μs pulse from a stimulation isolation unit controlled by a S48 pulse generator (Astro-Med, West Warwick, RI). A bipolar stimulating electrode (Frederick Haer Company, Bowdoinham, ME) was positioned ~100 μm from the neuron under recording. Before stimulation, cells (voltage clamped at −70 mV) were depolarized to +60 mV for 3 s to fully relieve the voltage-dependent Mg^{2+} block of NMDAR channels. The Clampfit Program (Axon Instruments) was used to analyze evoked synaptic activity. The amplitude of EPSC was calculated by taking the mean of a 2–4 ms window around the peak and comparing with the mean of a 4–8 ms window immediately before the stimulation artifact.

Antisense. To knock-down the expression of KIF17 (kinesin superfamily member 17) in cultured PFC neurons, we used the antisense oligonucleotide approach as described previously (Guillaud et al., 2003). The antisense oligonucleotide against KIF17 cDNA was 5′-CAGAGGC-

TCACCACCGAA-3′, and the corresponding sense oligonucleotide was 5′-TTCGGTGGTGAGCCTCTG-3′. To knock-down the expression of MAP2 (microtubule-associated protein 2) in cultured PFC neurons, we used the antisense oligonucleotide 5′-TCGTCAGCCATCCTTCAGATCTCT-3′ (Caceres et al., 1992). The MAP2 sense oligonucleotide 5′-AGAGATCTGAAGGATGGCTGACGA-3′ was used as a control. After 8–11 d of culture, a 1 μM concentration of oligonucleotides was added directly to the culture medium. Two to 3 d after being exposed to these oligonucleotides, electrophysiological recordings were performed on the cultured neurons.

Transfection. Cultured PFC neurons [11 d *in vitro* (DIV)] were cotransfected with a plasmid encoding the enhanced green fluorescent protein (EGFP) (Clontech, Cambridge, UK) and a plasmid containing either the wild-type MEK1 [wtMEK1 (mitogen-activated protein kinase kinase 1)] or the dominant-negative MEK1 (dnMEK1) (carrying M substitution at K97) construct (Kim et al., 2004). In some experiments, NR2B tagged with GFP at the extracellular N terminus (Luo et al., 2002) was used to transfect cultured PFC neurons. Transfection was conducted with the Lipofectamine 2000 method according to the protocol of the manufacturer (Invitrogen, San Diego, CA). Two to 3 d after transfection, recordings were performed on the GFP-positive neurons.

Small interfering RNA. To suppress the expression of CaMKII in cultured neurons, we used the small interfering RNA (siRNA), a potent agent for sequence-specific gene silencing (McManus and Sharp, 2002). The siRNA oligonucleotide sequences selected from α-CaMKII mRNA were 5′-GGAGUAUGCUGCCAAGAUUtt-3′ (sense) and 5′-AAUCUUGGCAGCAUACUCCtg-3′ (antisense). siRNA was synthesized (Ambion, Austin, TX) and cotransfected with EGFP into cultured PFC neurons (11 DIV) using the Lipofectamine 2000 method. Two to 3 d after transfection, immunocytochemical staining or electrophysiological recordings were performed.

Determination of microtubule stability. Free tubulin was extracted as described previously (Joshi and Cleveland, 1989). Cultured PFC neurons (14 DIV) in 3.5 cm dishes were washed twice with 1 ml of microtubule stabilizing buffer (0.1 M MES, pH 6.75, 1 mM $MgSO_4$, 2 mM EGTA, 0.1 mM EDTA, and 4 M glycerol). Cells were then incubated at 37°C for 5 min in 600 μl of soluble tubulin extraction buffer (0.1 M MES, pH 6.75, 1 mM $MgSO_4$, 2 mM EGTA, 0.1 mM EDTA, 4 M glycerol, and 0.1% Triton X-100) with the addition of protease inhibitor cocktail tablets (Roche Diagnostics, Indianapolis, IN). The soluble extract was centrifuged at 37°C for 2 min, and the supernatant was saved. Equal amount of protein was separated by 10% SDS-polyacrylamide gel. Western blot was performed using anti-α-tubulin (1:2000; Sigma) as the primary antibody. After Western blot, the tubulin bands were scanned and quantitatively analyzed with NIH Image.

Immunocytochemical staining. For the detection of CaMKII expression, after siRNA transfection, cultured neurons were fixed in 4% paraformaldehyde in PBS for 20 min and permeabilized with 0.3% Triton X-100 for 5 min. After 1 h of incubation with 10% bovine serum albumin (BSA) to block nonspecific staining, the cells were incubated with the monoclonal α-CaMKII antibody (1:200; Upstate Biotechnology, Lake Placid, NY) at 4°C overnight. For the detection of GFP-NR2B (Luo et al., 2002) on the cell surface, cultured neurons were treated with different agents after transfection, and then they were fixed in 4% paraformaldehyde but were not permeabilized. After background blocking in BSA, the cells were incubated with the anti-GFP antibody (1:100; Chemicon, Temecula, CA) at room temperature for 1 h. After washing off the primary antibodies, the cells were incubated with a rhodamine-conjugated secondary antibody (1:200; Sigma) for 50 min at room temperature. After washing in PBS three times, the coverslips were mounted on slides with Vectashield mounting media (Vector Laboratories, Burlingame, CA). Fluorescent images were obtained using a 60× objective with a cooled CCD camera mounted on a Nikon microscope.

The surface GFP-NR2B clusters were measured using Image J software. All specimens were imaged under identical conditions and analyzed using identical parameters. To define dendritic clusters, a single threshold was chosen manually, so that clusters corresponded to puncta of at least twofold greater intensity than the diffuse fluorescence on the dendritic shaft. Three to four independent experiments for each of the treatments were performed. On each coverslip, the cluster density, size, and fluorescence intensity of four to six neurons (two to three dendritic segments of at least 50 μm length per neuron) were measured. Quantitative analyses were conducted blindly (without knowledge of experimental treatment).

Results

Activation of 5-HT$_{1A}$ receptors reduces NMDAR-mediated ionic and synaptic currents in PFC pyramidal neurons and targets NR2B-containing NMDAR channels

To test the hypothesis that serotonin may be involved in cognitive and emotional processes by regulating NMDA signaling, we first examined the effect of 5-HT receptor activation on NMDA receptor-mediated currents in dissociated PFC pyramidal neurons. Our previous study has shown that 5-HT$_{1A}$ and 5-HT$_{2A}$ receptors are the most predominant serotonin receptor subtypes expressed in PFC pyramidal neurons (Feng et al., 2001); thus, we first examined the role of these receptors in regulating NMDA-evoked ionic currents. Application of 8-OH-DPAT (20 or 40 μM), a specific 5-HT$_{1A}$ receptor agonist, caused a significant reduction in the amplitude of NMDAR currents in acutely isolated PFC pyramidal neurons. The time course and current traces from a representative cell are shown in Figure 1, *A* and *B*. To verify that 5-HT$_{1A}$ receptors are mediating the serotonergic modulation of NMDAR currents, we examined the ability of selective 5-HT$_{1A}$ receptor antagonists to prevent the action of serotonin. As shown in Figure 1*C*, 5-HT (20 μM) produced a reversible reduction of NMDAR currents in the dissociated PFC neuron, similar to the effect of 8-OH-DPAT. Application of WAY-100635 (20 μM), a highly selective 5-HT$_{1A}$ antagonist, blocked the 5-HT reduction of NMDAR currents.

The effect of different agonists on peak NMDAR currents in the absence or presence of various antagonists is summarized in Figure 1*D*. 8-OH-DPAT had a potent inhibitory effect on both the peak and the steady state (ss) NMDAR currents in freshly isolated PFC neurons (peak, 21.2 ± 0.6%; ss, 17.7 ± 1.0%; $n = 183$; $p < 0.001$, Mann–Whitney *U* test). Fitting the NMDAR currents with single-exponential equations indicated that 8-OH-DPAT did not significantly alter the desensitization profile of NMDAR currents (τ in control, 0.53 ± 0.05 s; τ in 8-OH-DPAT, 0.59 ± 0.07 s; $n = 14$). A similar effect on the peak NMDAR currents was found in cultured PFC pyramidal neurons (24.7 ± 1.5%; $n = 30$; $p < 0.001$, Mann–Whitney *U* test). The 8-OH-DPAT- induced reduction of NMDAR currents was robust and reversible. After recovery from the first application, a second application of 8-OH-DPAT resulted in a similar response (96 ± 2.9% of first response; $n = 19$). The effect of 8-OH-DPAT was significantly attenuated by WAY-100635 (6.6 ± 1.4%; $n = 16$; $p > 0.05$, Mann–Whitney *U* test) or another highly selective 5-HT$_{1A}$ antagonist NAN-190 (20 μM; 5.5 ± 1.3%; $n = 4$; $p > 0.05$, Mann–Whitney *U* test). In contrast to the effect of 8-OH-DPAT, application of the specific 5-HT$_{2A/2C}$ agonist α-Me-5-HT (20 μM) had little effect on NMDAR currents (2.7 ± 0.9%; $n = 17$; $p > 0.05$, Mann–Whitney *U* test). Application of 5-HT produced a 17.1 ± 1.0% ($n = 19$; $p < 0.005$, Mann–Whitney *U* test) reduction of NMDAR currents, mimicking the effect of 8-OH-DPAT. Moreover, 5-HT failed to produce a significant effect on NMDAR currents in the presence of the nonselective 5-HT receptor antagonist methysergide (20 μM; 1.5 ± 0.7%; $n = 5$; $p > 0.05$, Mann–Whitney *U* test) or the selective 5-HT$_{1A}$ antagonist WAY-100635 (2.8 ± 0.9%; $n = 6$; $p > 0.05$, Mann–Whitney *U* test). The pharmacological data thus suggest that serotonin re-

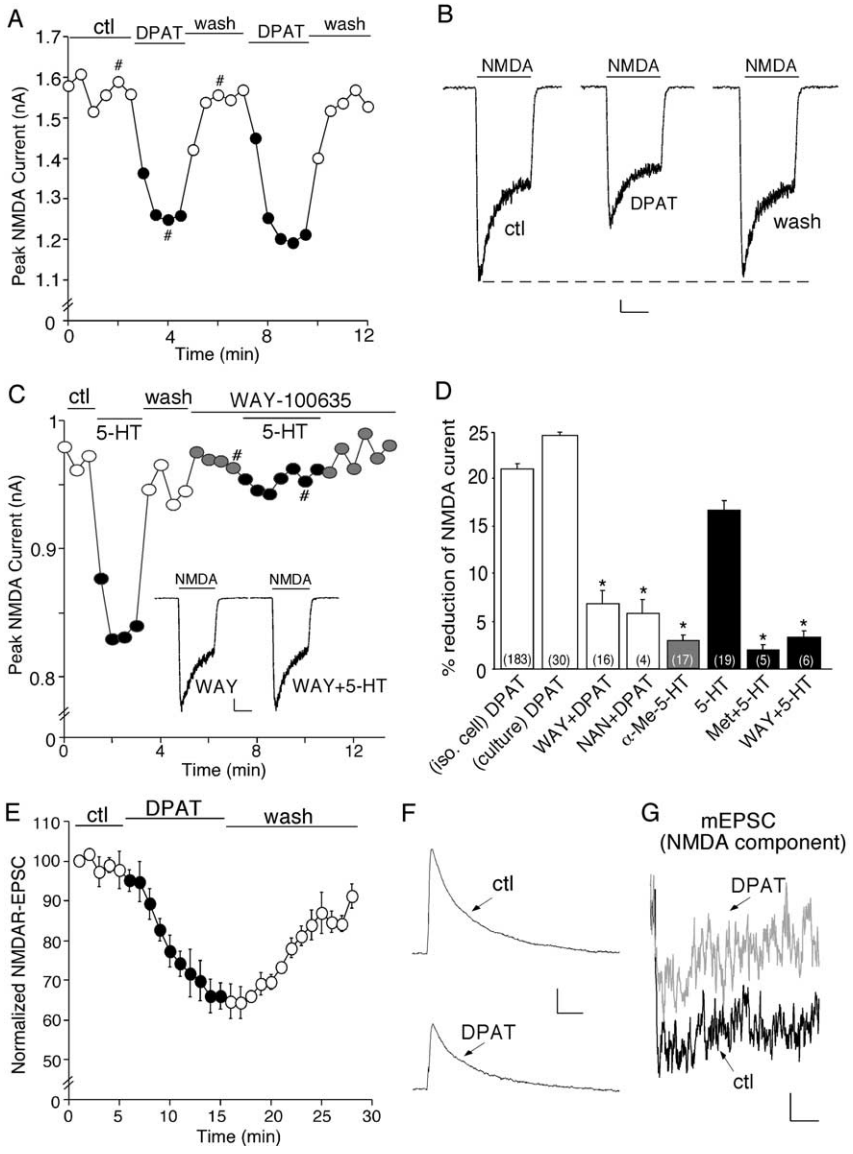

Figure 1. Activation of 5-HT$_{1A}$ receptors reversibly reduces NMDA receptor-mediated ionic and synaptic currents in PFC pyramidal neurons. ***A***, Plot of peak NMDAR currents showing that the 5-HT$_{1A}$ agonist 8-OH-DPAT (DPAT; 40 μM) decreased NMDA (100 μM)-evoked currents in the dissociated neuron. ***B***, Representative current traces taken from the records used to construct ***A*** (at time points denoted by #). Calibration: 100 pA, 1 s. ***C***, Plot of peak NMDAR currents showing that 5-HT (20 μM) decreased NMDAR currents but failed to do so in the presence of the 5-HT$_{1A}$ antagonist WAY-100635 (WAY; 20 μM). Inset, Representative current traces (at time points denoted by #). Calibration: 100 pA, 1 s. ***D***, Cumulative data (mean ± SEM) showing the percentage reduction of NMDAR currents by different agonists in the absence or presence of various antagonists. The number of cells tested in each condition is shown in each bar. *$p < 0.005$, ANOVA. ***E***, Plot of normalized peak evoked NMDAR EPSCs as a function of time and agonist (8-OH-DPAT, 20 μM) application in a sample of neurons tested. Each point represents the average peak (mean ± SEM) of three consecutive NMDAR EPSCs. ***F***, Representative current traces (average of 3 trials) taken from the records used to construct ***E*** (at time points denoted by #). Calibration: 100 pA, 100 ms. ***G***, Representative averaged mEPSCs (NMDAR component) obtained in the absence (ctl) or presence of 8-OH-DPAT (40 μM). Calibration: 0.5 pA, 40 ms. NAN, NAN-190; iso. cell, isolated cell; Met, methysergide; ctl, control.

leased on PFC pyramidal neurons could indeed modulate NMDA receptors via the activation of 5-HT$_{1A}$ receptors.

Because the NMDA-evoked current in isolated neurons is mediated by both synaptic and extrasynaptic NMDA receptors, we further examined the effect of 5-HT$_{1A}$ receptors on NMDAR EPSCs evoked by stimulation of synaptic NMDA receptors in PFC slices. As shown in Figure 1, *E* and *F*, application of 8-OH-DPAT induced a significant reduction in the amplitude of NMDAR EPSCs. In parallel control measurements in which no 8-OH-DPAT was administrated, NMDAR EPSCs remained stable throughout the length of the recording (data not shown). In a sample of PFC pyramidal neurons we examined, 8-OH-DPAT decreased the mean amplitude of NMDAR EPSCs by 37.6 ± 3.6% ($n = 17$; $p < 0.001$, Mann–Whitney *U* test).

To further confirm the impact of 8-OH-DPAT on postsynaptic NMDA receptors, we also measured mEPSCs in cultured PFC pyramidal neurons exposed to TTX (1 μM). mEPSCs result from the random release of single neurotransmitter packets (quanta), and a significant effect on their amplitude reflexes a modification of postsynaptic glutamate receptors. The NMDAR component of mEPSC was obtained by subtracting the AMPAR component (recorded in the presence of D-APV and Mg^{2+}) from the total mEPSCs (recorded in Mg^{2+}-free solutions). As shown in the representative experiment (Fig. 1*G*), 8-OH-DPAT caused a potent reduction of the amplitude of NMDAR mEPSC. In a sample of neurons tested, 8-OH-DPAT decreased the NMDAR component of mEPSCs by 35.3 ± 4.4% ($n = 8$; $p < 0.001$, Mann–Whitney *U* test).

In mature cortical synapses, the primary NMDA receptors, which are composed of NR1/NR2A or NR1/NR2B, differ in subcellular localization (Vicini et al., 1998; Cull-Candy et al., 2001). NR2A-containing NMDA receptors are mainly concentrated at postsynaptic densities (PSDs) of dendritic spines, whereas NR2B-containing NMDA receptors are located at both synaptic and extrasynaptic sites of dendritic shafts and spines (Li et al., 1998; Tovar and Westbrook, 1999). To determine which subpopulation(s) of NMDARs is modulated by 5-HT$_{1A}$ receptors, we applied the selective inhibitor of NR2B subunit ifenprodil (Williams, 1993). Blocking NR2B subunit-containing NMDARs with ifenprodil (3 μM) reduced the amplitude of NMDAR currents by 53.3 ± 2.0% in acutely isolated PFC pyramidal neurons ($n = 14$). In the presence of ifenprodil, 8-OH-DPAT had almost no effect on the remaining NMDAR currents (Fig. 2*A*,*B*). In a sample of freshly isolated (3-week-old) neurons ($n = 14$) and cultured (12 DIV) neurons ($n = 7$) we tested, ifenprodil significantly blocked the effect of 8-OH-DPAT (Fig. 2*C*), suggesting that 5-HT$_{1A}$ receptors primarily target NR2B subunit-containing NMDA receptors.

The 5-HT$_{1A}$ modulation of NMDA receptors is dependent on microtubule stability and involves the transport of NR2B-containing vesicles along microtubules by the kinesin motor protein KIF17

We next examined the potential mechanism underlying the reduction of NMDAR currents by 8-OH-DPAT. The trafficking of NMDA receptors has been considered to play a key role in regu-

lating the function of these channels at the cell membrane (Carroll and Zukin, 2002; Wenthold et al., 2003). After NMDA receptors comprising NR1 and NR2 subunits leave the endoplasmic reticulum (ER), they are further processed in the cell body and then transported along microtubules in dendrites to the synapse. Thus, we hypothesize that one possible mechanism for the 8-OH-DPAT reduction of NMDAR currents could be attributable to the 5-HT$_{1A}$-induced interference of NMDA receptor transport along microtubules in dendrites. To test this, we examined the effect of 8-OH-DPAT in the presence of agents that depolymerize or stabilize microtubules. As shown in Figure 3*A*, application of the microtubule-depolymerizing agent nocodazole (30 μM) suppressed NMDAR currents, mimicking the effect of 8-OH-DPAT. Colchicine (30 μM), another microtubule-depolymerizing agent, caused a similar inhibition of NMDAR currents (data not shown). Subsequent application of 8-OH-DPAT in the presence of nocodazole failed to produce an additional effect on NMDAR currents. Conversely, taxol (10 μM), a microtubule-stabilizing agent, abolished the effect of 8-OH-DPAT on NMDAR currents (Fig. 3*B*).

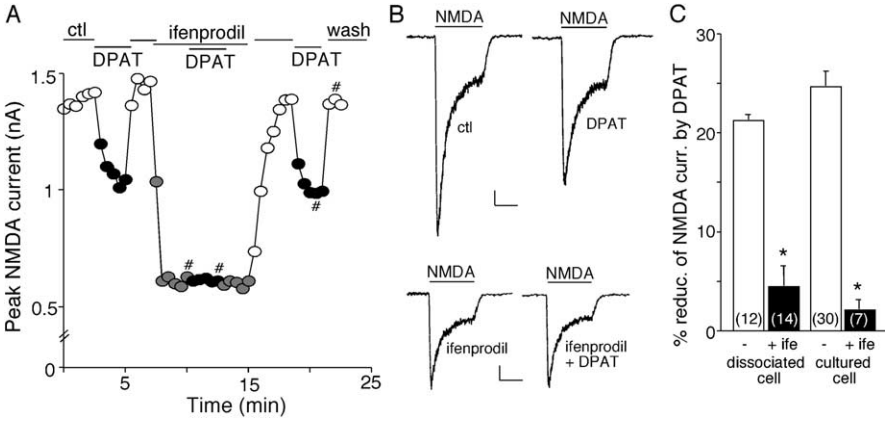

Figure 2. Activation of 5-HT$_{1A}$ receptors targets NR2B-containing NMDAR channels. ***A***, Plot of peak NMDAR currents showing the effect of 8-OH-DPAT (DPAT; 40 μM) in the absence or presence of ifenprodil (3 μM), the selective inhibitor of NR2B subunit, in a PFC pyramidal neuron freshly isolated from a 3-week-old rat. ***B***, Representative current traces taken from the records used to construct ***A*** (at time points denoted by #). Calibration: 100 pA, 1 s. ***C***, Cumulative data (mean ± SEM) showing the percentage reduction of NMDAR currents by 8-OH-DPAT in the absence (ctl) or presence of ifenprodil (ife) in a sample of acutely dissociated or cultured neurons. The number of cells tested in each condition is shown in each bar. *$p < 0.005$, ANOVA. ctl, Control.

To determine whether the 5-HT$_{1A}$ modulation of NMDAR currents is affected by the integrity of F-actin, we used the potent actin-depolymerizing agent latrunculin B. As shown in Figure 3*C*, application of latrunculin (5 μM) resulted in a gradual decrease of NMDAR current, consistent with previous results (Rosenmund and Westbrook, 1993). However, subsequent application of 8-OH-DPAT in the presence of latrunculin still induced a marked reduction of NMDAR currents, indicating that latrunculin did not occlude the effect of 8-OH-DPAT. To further test the involvement of actin cytoskeleton, we dialyzed neurons with phalloidin (4 μM), an actin-stabilizing compound. As shown in Figure 3*D*, the 8-OH-DPAT reduction of NMDAR currents was not prevented when actin filaments were stabilized by phalloidin.

The effect of 8-OH-DPAT on NMDAR currents in the absence or presence of various agents that alter microtubule or actin depolymerization are summarized in Figure 3*E*. In a sample of acutely isolated or cultured PFC pyramidal neurons we tested, nocodazole reduced NMDAR currents by 23.1 ± 2.0% ($n = 11$; $p < 0.001$, Mann–Whitney *U* test). A similar effect was found with colchicine (22.3 ± 1.9%; $n = 13$; $p < 0.001$, Mann–Whitney *U* test). 8-OH-DPAT produced little reduction of NMDAR currents in the presence of nocodazole (6.0 ± 1.4%; $n = 6$; $p > 0.05$, Mann–Whitney *U* test) or colchicine (6.0 ± 1.2%; $n = 6$; $p > 0.05$, Mann–Whitney *U* test), whereas 8-OH-DPAT significantly reduced NMDAR currents in the absence of these agents (23.1 ± 1.0%; $n = 26$; $p < 0.001$, Mann–Whitney *U* test), indicating that both microtubule depolymerizers occluded the effect of 8-OH-DPAT. Moreover, taxol itself had little effect on NMDAR currents (5.7 ± 1.3%; $n = 13$; $p > 0.05$, Mann–Whitney *U* test), whereas 8-OH-DPAT caused little suppression of NMDAR currents in the presence of taxol (6.7 ± 0.7%; $n = 6$; $p > 0.05$, Mann–Whitney *U* test), indicating that the microtubule stabilizer blocked the effect of 8-OH-DPAT. The actin-depolymerizing agent latrunculin caused a 24.1 ± 2.0% ($n = 11$; $p < 0.001$, Mann–Whitney *U* test) decrease of NMDAR currents, but 8-OH-DPAT still significantly decreased NMDAR currents in the presence of latrunculin (24.2 ± 3.0%; $n = 6$; $p < 0.001$, Mann–Whitney *U* test). Similarly, the effect of 8-OH-DPAT was also intact in cells loaded with phalloidin (28.0 ± 3.4%; $n = 5$; $p < 0.001$, Mann–Whitney *U* test), indicating that the effect of 8-OH-DPAT was not dependent on the depolymerization of actin filaments. Together, these results suggest that 5-HT$_{1A}$ receptors regulate NMDAR currents by interfering with the transport of NMDA receptors along microtubules.

To test whether clathrin-dependent endocytosis of NMDA receptors (Vissel et al., 2001; Nong et al., 2003) is also involved in the 5-HT$_{1A}$ modulation of NMDAR currents, we dialyzed neurons with a dynamin inhibitory peptide that interferes with the binding of amphiphysin with dynamin and therefore prevents endocytosis through clathrin-coated pits (Grabs et al., 1997; Marks and McMahon, 1998). We found that the effect of 8-OH-DPAT was intact in neurons loaded with the dynamin inhibitory peptide (50 μM; 21.5 ± 2.1%; $n = 4$) (Fig. 3*E*), which rules out the involvement of clathrin-mediated endocytosis in the 5-HT$_{1A}$ modulation of NMDAR currents.

Transport of NMDARs along microtubules in dendrites requires the kinesin motor protein KIF17, which is linked to NR2B-containing vesicles (Setou et al., 2000). To test whether the KIF17-mediated transport of NMDA receptors along microtubules is involved in the 5-HT$_{1A}$ regulation of NMDAR currents, we performed cellular knock-down of KIF17 by treatment of PFC cultures with antisense oligonucleotides (Guillaud et al., 2003) and examined the effect of 8-OH-DPAT on NMDAR currents in these cultures. It has been shown that KIF17 antisense oligonucleotides, but not sense oligonucleotides, totally inhibited KIF17 expression (Guillaud et al., 2003). We found that, in cultured PFC neurons treated with KIF17 antisense oligonucleotides (1 μM), the basal whole-cell NMDAR currents were reduced (control, 1122.2 ± 92.8 pA, $n = 10$; KIF antisense, 546.7 ± 36.7 pA, $n = 23$), but the selective inhibitor of NR2B subunit ifenprodil (3 μM) reduced NMDAR currents by 63.8 ± 3.5% ($n = 11$), similar to the effect of ifenprodil in nontreated cultures (70.8 ± 2.3%; $n = 18$), suggesting that the composition of NMDA receptor subunits was not significantly altered by KIF17 downregulation. However, 8-OH-DPAT had little effect on NMDAR currents in

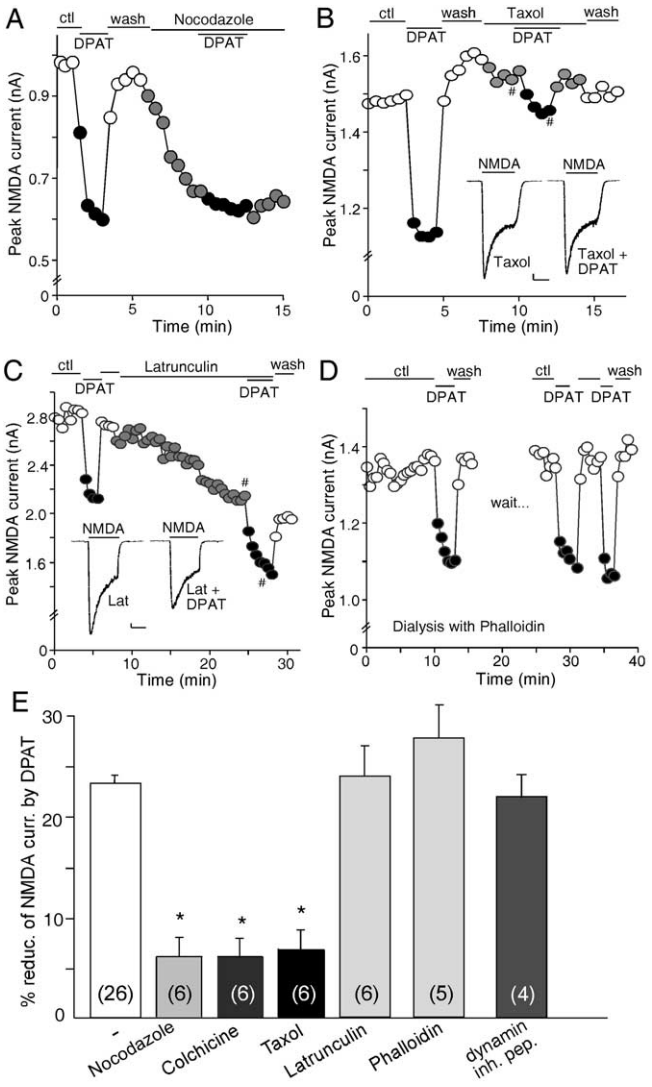

Figure 3. The 5-HT$_{1A}$ effect on NMDAR currents is dependent on microtubule stability but not actin cytoskeleton or the clathrin-mediated endocytosis of NMDA receptors. ***A***, Plot of peak NMDAR currents showing that the effect of 8-OH-DPAT (DPAT) was mimicked and occluded by the microtubule-depolymerizing agent nocodazole (30 μM). ***B***, Plot of peak NMDAR currents showing that the microtubule-stabilizing agent taxol (10 μM) blocked the effect of 8-OH-DPAT. Inset, Representative current traces (at time points denoted by #). Calibration: 100 pA, 1 s. ***C***, Plot of peak NMDAR currents showing that the actin-depolymerizing agent latrunculin B (Lat; 5 μM) failed to occlude the effect of 8-OH-DPAT. Inset, Representative current traces (at time points denoted by #). Calibration: 100 pA, 1 s. ***D***, Plot of peak NMDAR currents showing that dialysis with the actin-stabilizing agent phalloidin (4 μM) did not block the effect of 8-OH-DPAT. ***E***, Cumulative data (mean ± SEM) showing the percentage reduction of NMDAR currents by 8-OH-DPAT in the absence (ctl) or presence of various agents that interfere with the microtubule or actin network, or a dynamin inhibitory peptide (inh. pep.; 50 μM). The number of cells tested in each condition is shown in each bar. *$p < 0.005$, ANOVA. ctl, Control.

neurons exposed to KIF17 antisense oligonucleotides, whereas the effect of 8-OH-DPAT was intact in neurons exposed to KIF17 sense oligonucleotides (1 μM) (Fig. 4*A*,*B*). As summarized in Figure 4*C*, 8-OH-DPAT produced little reduction of NMDAR currents in cultured neurons treated with KIF17 antisense oligonucleotides (4.2 ± 0.6%; $n = 23$; $p > 0.05$, Mann–Whitney *U* test), which was significantly different from the effect of 8-OH-DPAT in cultured neurons treated with KIF17 sense oligonucleotides (22.8 ± 2.0%; $n = 6$; $p < 0.001$, Mann–Whitney *U* test). These results suggest that the 5-HT$_{1A}$ modulation of NMDAR currents involves the transport of NR2B-containing NMDA receptors along microtubules in dendrites by the motor protein KIF17.

Given the microtubule dependence of the 5-HT$_{1A}$ modulation of NMDAR currents, we wanted to know how the 5-HT$_{1A}$ signaling affects microtubule stability. One possible mechanism is to change the phosphorylation state of MAP2, a microtubule-associated protein that is dendrite specific (Bernhardt and Matus, 1984; Caceres et al., 1984), therefore altering the association of MAP2 with microtubules and microtubule stability (Brugg and Matus 1991; Sanchez et al., 2000). To test this, we inhibited the expression of MAP2 by treating PFC cultures (8–11 DIV) with MAP2 antisense oligonucleotides (Caceres et al., 1992) and examined the 5-HT$_{1A}$ effect on NMDAR currents. No major changes were found on dendritic morphology in MAP2 antisense-treated neurons. The basal NMDAR currents were also unaltered (MAP2 antisense, 1085.7 ± 103.4 pA, $n = 7$; control, 1122.2 ± 92.8 pA, $n = 10$). As shown in Figure 4, *D* and *E*, 8-OH-DPAT failed to modulate NMDAR currents in the neuron in which MAP2 expression was suppressed by MAP2 antisense oligonucleotides (1 μM), whereas the effect of 8-OH-DPAT was intact in the neuron exposed to vehicle control. As summarized in Figure 4*F*, in cultured neurons treated with MAP2 antisense oligonucleotides, 8-OH-DPAT reduced NMDAR currents by 6.4 ± 1.3% ($n = 7$; $p > 0.05$, Mann–Whitney *U* test), which was significantly smaller than the effect of 8-OH-DPAT in vehicle control neurons (26.1 ± 2.6%; $n = 7$; $p < 0.001$, Mann–Whitney *U* test) or neurons treated with MAP2 sense oligonucleotides (26.6 ± 1.4%; $n = 5$; $p < 0.001$, Mann–Whitney *U* test), suggesting the involvement of MAP2 in the 5-HT$_{1A}$ modulation of NMDAR currents.

Regulating the activity of CaMKII and ERK, both of which are downstream of PKA, is essential for the 5-HT$_{1A}$ modulation of NMDA receptors

Because the 5-HT$_{1A}$ modulation of NMDAR currents depends on the regulation of MAP2 and microtubule stability, we wanted know what molecules link 5-HT$_{1A}$ receptors to the MAP2–microtubule complex. Two protein kinases known to phosphorylate MAP2 in the microtubule binding domain are CaMKII (Schulman, 1984) and ERK1/2 (Ray and Sturgill, 1987). We then examined whether CaMKII and/or ERK was important for the 5-HT$_{1A}$ modulation of NMDAR currents.

To test the role of CaMKII, we first used two agents that specifically inhibit CaMKII via different mechanisms, KN-93 and the AIP. As shown in Figure 5*A*, in the presence of KN-93 (20 μM), but not its inactive analog KN-92 (10 μM), 8-OH-DPAT lost the capability to regulate NMDAR currents. As summarized in Figure 5*B*, 8-OH-DPAT had little effect on NMDAR currents in the presence of KN-93 (3.1 ± 0.6%; $n = 15$; $p > 0.05$, Mann–Whitney *U* test), which was significantly different from the effect of 8-OH-DPAT in the absence of the CaMKII inhibitor (21.7 ± 0.9%; $n = 60$; $p < 0.001$, Mann–Whitney *U* test) or in the presence of KN-92 (15 ± 0.8%; $n = 6$; $p < 0.005$, Mann–Whitney *U* test). The 8-OH-DPAT-induced suppression of NMDAR currents was also abolished by bath application of the myristoylated AIP peptide (0.5 μM; 2.2 ± 0.8%; $n = 8$; $p > 0.05$, Mann–Whitney *U* test) or dialysis with the AIP peptide (5 μM; 2.5 ± 0.5%; $n = 7$; $p > 0.05$, Mann–Whitney *U* test). Dialysis with purified calmodulin (10 μM) or the calmodulin antagonist CDZ (10 μM) or the calmodulin inhibitory peptide (MLCKP, 20 μM) was unable to block the 8-OH-DPAT reduction of NMDAR currents (calmodulin, 18.3 ± 0.6%, $n = 8$; CDZ, 26.4 ± 1.3%, $n = 5$; MLCKP, 24.4 ± 2.2%, $n = 7$; $p < 0.001$, Mann–Whitney *U* test)

(Fig. 5*B*), suggesting the lack of involvement of Ca^{2+}/calmodulin-dependent inactivation of NMDARs (Zhang et al., 1998; Chen et al., 2004) in the 5-HT$_{1A}$ modulation of NMDA receptors.

To further confirm the involvement of CaMKII, we suppressed CaMKII protein expression in cultured PFC neurons by transfecting an siRNA directed against CaMKII. GFP was cotransfected with CaMKII siRNA, and the expression of CaMKII was detected with the immunocytochemical approach. We found that, in all of the GFP-positive neurons we observed, the transfected CaMKII siRNA markedly abolished the expression of CaMKII (n = 18). A representative example is shown in Figure 5*C* (top). Without the cotransfection of CaMKII siRNA, the expression of CaMKII was intact in GFP-positive neurons (Fig. 5*C*, bottom).

Because the CaMKII siRNA has caused efficient and specific downregulation of CaMKII expression, it is likely to cause functional inactivation of CaMKII. Thus, we examined the 5-HT$_{1A}$ modulation of NMDA receptors in CaMKII siRNA-transfected neurons. As controls, neurons were transfected with GFP alone or a scrambled siRNA. The basal whole-cell NMDAR currents were smaller in CaMKII siRNA-transfected neurons (601.5 ± 30.7 pA; n = 10) compared with scrambled siRNA-transfected neurons (990 ± 18.7 pA; n = 5). As shown in Figure 5*D*, 8-OH-DPAT had little effect on NMDAR currents in the GFP-positive neuron transfected with CaMKII siRNA, although it produced a potent reduction of NMDAR currents in the control neuron transfected with GFP alone. As summarized in Figure 5*E*, in cultured neurons transfected with CaMKII siRNA, 8-OH-DPAT reduced NMDAR currents by 5.1 ± 0.8% (n = 10; $p > 0.05$, Mann–Whitney U test), which was significantly smaller than the effect of 8-OH-DPAT in control neurons without CaMKII siRNA transfection (24.7 ± 1.5%; n = 9; $p < 0.001$, Mann–Whitney U test) or in neurons transfected with a scrambled siRNA (22.8 ± 2.1%; n = 5; $p < 0.001$, Mann–Whitney U test). Together, these results suggest that CaMKII is involved in the 5-HT$_{1A}$ modulation of NMDAR currents.

We then tested the role of ERK in the 5-HT$_{1A}$ modulation of NMDAR currents. First, we used two structurally and mechanistically distinct inhibitors of MEK (the kinase upstream of ERK), U0126 and PD98059. As shown in Figure 6, *A* and *B*, in the presence of U0126 (20 μM), 8-OH-DPAT failed to modulate NMDAR currents. To further confirm the involvement of ERK, we blocked the activity of ERK by overexpression of a dnMEK1 that is catalytically inactive (Mansour et al., 1994). As shown in Figure 6, *C* and *D*, in the cultured neuron transfected with dnMEK1, 8-OH-DPAT had little effect on NMDAR currents, whereas in the cultured neuron transfected with wtMEK1, 8-OH-DPAT produced a marked reduction of NMDAR currents, similar to what was found in nontransfected neurons. As summarized in Figure 6*E*, in the presence of U0126 or PD98059 (40 μM), 8-OH-DPAT produced little reduction of NMDAR currents (U0126, 3.5 ± 1.0%, n = 12; PD98059, 4.3 ± 0.7%, n = 13; $p > 0.05$, Mann–Whitney U test), which was significantly different from the effect of 8-OH-DPAT under control conditions (23.7 ± 1.3%; n = 42; $p < 0.001$, Mann–Whitney U test), indicating that both MEK inhibitors prevented the 5-HT$_{1A}$ modulation of NMDAR currents. In addition, the effect of 8-OH-DPAT in dnMEK1-transfected neurons (5.5 ± 0.7%; n = 13; $p > 0.05$, Mann–Whitney U test) was significantly smaller than that in wtMEK1-transfected neurons (24 ± 2.8%; n = 6; $p < 0.001$, Mann–Whitney U test), further confirming the involvement of ERK in the 5-HT$_{1A}$ modulation of NMDAR currents.

Next, we tried to determine how activation of 5-HT$_{1A}$ receptors triggers the change of CaMKII and ERK activity, which subsequently alters microtubule activity and leads to the reduced NMDA receptor transport along microtubules. A classic pathway for 5-HT$_{1A}$ receptors is to couple to G_i/G_o-proteins to inhibit adenylate cyclase and cAMP formation (Raymond et al., 1999).

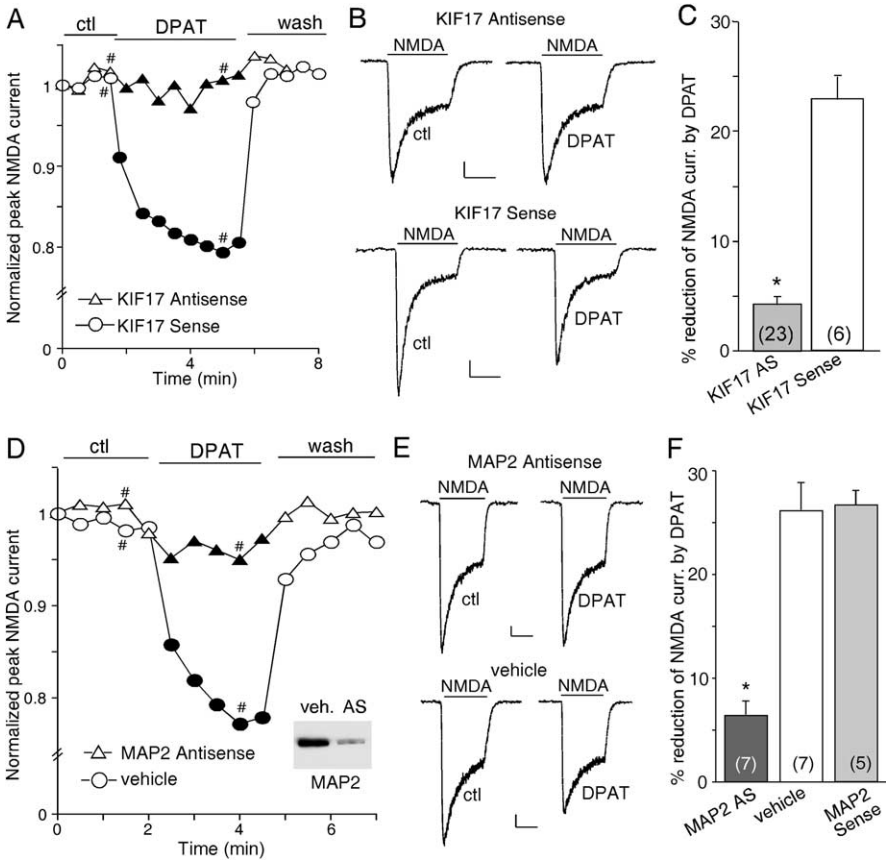

Figure 4. The 5-HT$_{1A}$ modulation of NMDAR currents involves the transport of NR2B-containing vesicles along microtubules by the kinesin motor protein KIF17 and requires the microtubule-binding protein MAP2. ***A***, Plot of peak NMDAR currents as a function of time and agonist [8-OH-DPAT (DPAT), 20 μM] application in neurons treated with KIF17 antisense or sense oligonucleotides. ***B***, Representative current traces taken from the records used to construct ***A*** (at time points denoted by #). Calibration: 100 pA, 1 s. ***C***, Cumulative data (mean ± SEM) showing the percentage reduction of NMDAR currents by 8-OH-DPAT in a sample of cultured neurons treated with KIF17 antisense or sense oligonucleotides. ***D***, Plot of peak NMDAR currents as a function of time and 8-OH-DPAT (40 μM) application in neurons treated with MAP2 antisense oligonucleotides or vehicle control. Inset, Western blot analysis of MAP2 expression in cultured PFC neurons treated with vehicle (veh.) or MAP2 antisense oligonucleotides (AS). ***E***, Representative current traces taken from the records used to construct ***D*** (at time points denoted by #). Calibration: 100 pA, 1 s. ***F***, Cumulative data (mean ± SEM) showing the percentage reduction of NMDAR currents by 8-OH-DPAT in a sample of cultured neurons treated with MAP2 antisense oligonucleotides, vehicle control, or MAP2 sense oligonucleotides. The number of cells tested in each condition is shown in each bar (***C***, ***F***). *$p < 0.005$, ANOVA. ctl, Control.

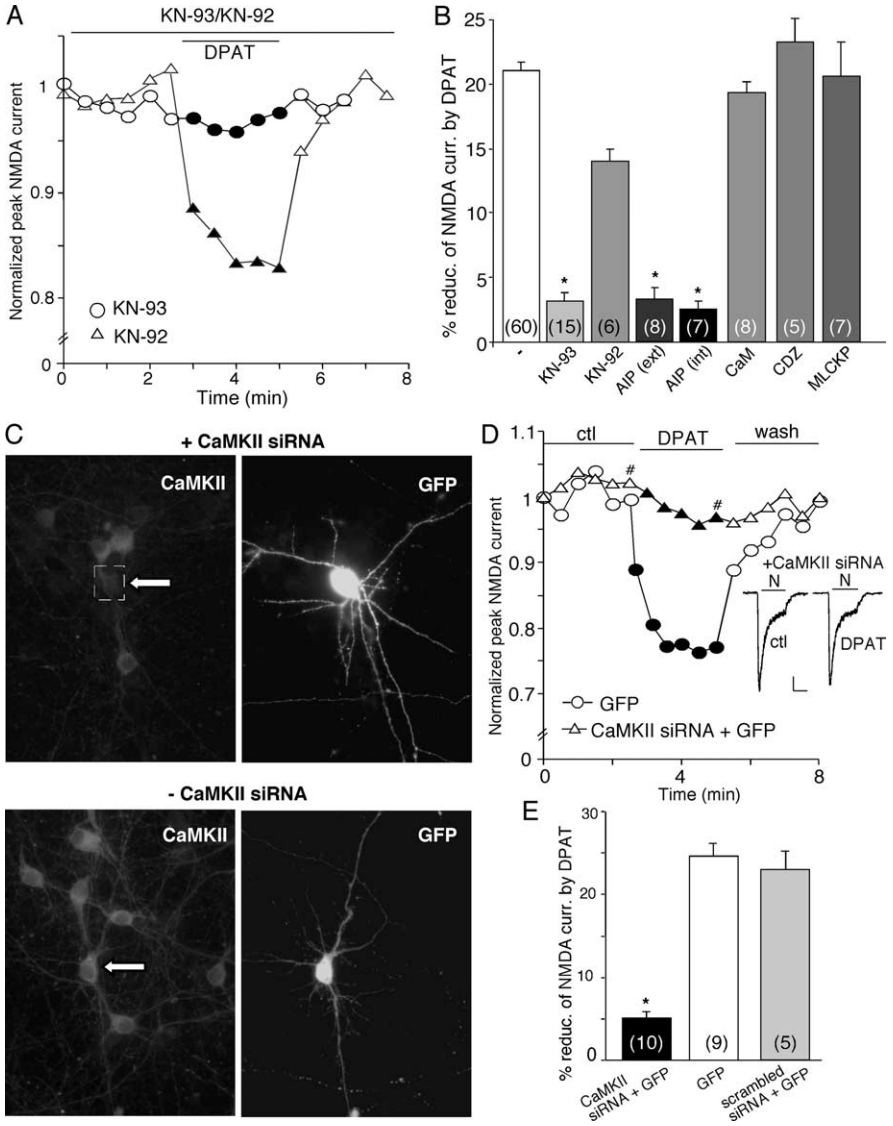

Figure 5. Inhibition of CaMKII prevents the 5-HT$_{1A}$ reduction of NMDAR currents. ***A***, Plot of peak NMDAR currents showing that the CaMKII inhibitor KN-93 (20 μM), but not its inactive analog KN-92 (10 μM), prevented 8-OH-DPAT (DPAT; 40 μM) from reducing NMDAR currents. ***B***, Cumulative data (mean ± SEM) showing the percentage reduction of NMDAR currents by 8-OH-DPAT in the absence (ctl) or presence of various agents that affect CaMKII or calmodulin. The number of cells tested in each condition is shown in each bar. *$p < 0.005$, ANOVA. ext, External; int, internal. ***C***, Immunocytochemical images stained with anti-α-CaMKII in cultured neurons cotransfected with CaMKII siRNA and GFP (top) or transfected with GFP alone (bottom). Note that CaMKII siRNA suppressed the expression of CaMKII in the GFP-positive neuron. Arrows indicate GFP-positive cells. ***D***, Plot of peak NMDAR currents as a function of time and agonist (8-OH-DPAT, 20 μM) application in a GFP-positive neuron transfected with CaMKII siRNA and a GFP-positive neuron without CaMKII siRNA transfection. Inset, Representative current traces (at time points denoted by #). Calibration: 100 pA, 1 s. ***E***, Cumulative data (mean ± SEM) showing the percentage reduction of NMDAR currents by 8-OH-DPAT in a sample of GFP-positive neurons transfected with or without CaMKII siRNA or with a scrambled siRNA. The number of cells tested in each condition is shown in each bar. *$p < 0.005$, ANOVA. ctl, Control.

This led us to speculate that the 5-HT$_{1A}$ reduction of NMDAR currents is through the inhibition of PKA, which results in the inhibition of CaMKII via the I-1/protein phosphatase 1 (PP1) cascade (Ingebritsen and Cohen, 1983; Miller and Kennedy, 1986; Cai et al., 2002), and the inhibition of ERK via the Rap1/B-Raf/MEK cascade (Vossler et al., 1997; Roberson et al., 1999). If that is the case, then the effect of 5-HT$_{1A}$ on NMDAR currents should be blocked by stimulating PKA and occluded by inhibiting PKA. To test this, we applied selective PKA activators and inhibitors.

As shown in Figure 7*A*, application of the membrane-permeable PKA activator cpt-cAMP (50 μM) blocked the effect of 8-OH-DPAT. Removing cpt-cAMP restored the ability of 8-OH-DPAT to modulate NMDAR currents. In addition, dialysis neurons with the specific PKA inhibitory peptide PKI[5–24] (40 μM) prevented 8-OH-DPAT from reducing NMDAR currents (Fig. 7*B*). As summarized in Figure 7*C*, 8-OH-DPAT produced little effect on NMDA receptor currents in the presence of cpt-cAMP (1.7 ± 0.5%; $n = 7$; $p > 0.05$, Mann–Whitney *U* test), PKI[5–24] (5 ± 1.5%; $n = 8$; $p > 0.05$, Mann–Whitney *U* test), or the myristoylated PKA inhibitory peptide PKI$_{14-22}$ (2.2 ± 0.7%; $n = 9$; $p > 0.05$, Mann–Whitney *U* test), all of which were significantly smaller than the effect of 8-OH-DPAT in the absence of these agents (21.2 ± 0.9%; $n = 25$; $p < 0.001$, Mann–Whitney *U* test). These results indicate that the 5-HT$_{1A}$ reduction of NMDAR currents depends on the inhibition of PKA.

To test the involvement of the I-1/PP1 cascade, which is upstream of CaMKII, in the 5-HT$_{1A}$/PKA regulation of NMDAR currents, we also examined the effect of 8-OH-DPAT on NMDAR currents in the presence of PP1 inhibitors. Dialysis with the PP1/2A inhibitor OA (1 μM) significantly attenuated the ability of 8-OH-DPAT to inhibit NMDAR currents (5.8 ± 1.7%; $n = 6$; $p > 0.05$, Mann–Whitney *U* test) (Fig. 7*C*). Loading cells with phosphorylated I-1 peptide p^{Thr35}I-1[7–39] (40 μM), a potent and selective PP1 inhibitor (Foulkes et al., 1983), also markedly blocked the effect of 8-OH-DPAT (5.7 ± 0.8%; $n = 7$; $p > 0.05$, Mann–Whitney *U* test) (Fig. 7*C*).

As controls, we also examined the potential involvement of the phospholipid cascade in 5-HT$_{1A}$ regulation of NMDAR currents (Fig. 7*D*). Application of the phospholipase C (PLC) inhibitor U73122 (10 μM) failed to block the 8-OH-DPAT-induced reduction of NMDAR currents (25.6 ± 2.3%; $n = 9$; $p < 0.001$, Mann–Whitney *U* test). Similarly, the effect of 8-OH-DPAT was intact in the presence of the membrane-permeable IP$_3$ receptor antagonist 2APB (15 μM; 29.7 ± 2.1%; $n = 5$; $p < 0.001$, Mann–Whitney *U* test) or the specific PKC inhibitor calphostin C (1 μM; 17.5 ± 1.9%; $n = 6$; $p < 0.005$, Mann–Whitney *U* test). These data indicate that the PLC/IP$_3$/PKC signaling is not involved in the 5-HT$_{1A}$ regulation of NMDAR currents.

Activation of 5-HT$_{1A}$ receptors deceases microtubule stability through a mechanism involving CaMKII and ERK

The aforementioned electrophysiological evidence has suggested that 5-HT$_{1A}$ receptors regulate NMDAR currents through a microtubule-dependent mechanism; therefore, we wanted to

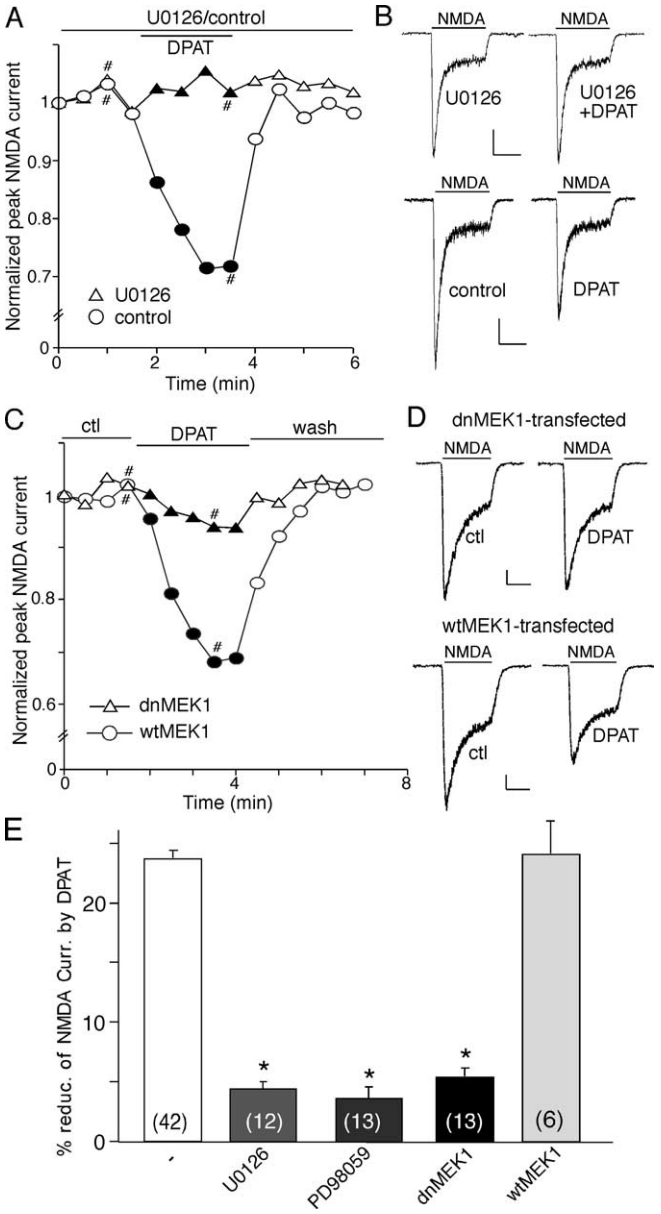

Figure 6. Inhibition of ERK prevents the 5-HT$_{1A}$ reduction of NMDAR currents. ***A***, Plot of peak NMDAR currents showing that 8-OH-DPAT (DPAT; 40 μM) failed to modulate NMDAR currents in the presence of the MEK inhibitor U0126 (20 μM). ***B***, Representative current traces taken from the records used to construct ***A*** (at time points denoted by #). Calibration: 100 pA, 1 s. ***C***, Plot of peak NMDAR currents as a function of time and agonist (8-OH-DPAT, 20 μM) application in a GFP-positive neuron transfected with dnMEK1 and a GFP-positive neuron transfected with wtMEK1. ***D***, Representative current traces taken from the records used to construct ***C*** (at time points denoted by #). Calibration: 100 pA, 1 s. ***E***, Cumulative data (mean ± SEM) showing the percentage reduction of NMDAR currents by 8-OH-DPAT in a sample of neurons in the absence (ctl) or presence of different MEK inhibitors, as well as in a sample of GFP-positive neurons transfected with dnMEK1 or wtMEK1. The number of cells tested in each condition is shown in each bar. *$p < 0.005$, ANOVA. ctl, Control.

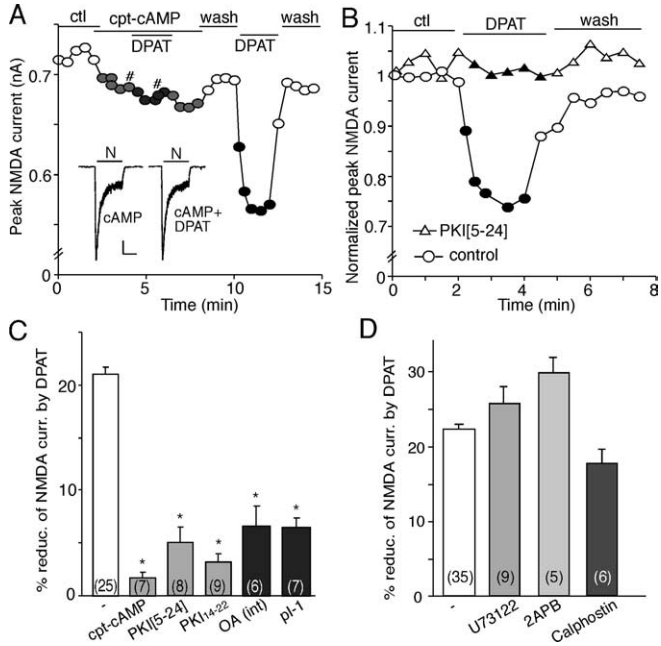

Figure 7. The 5-HT$_{1A}$ reduction of NMDAR currents requires the inhibition of PKA. ***A***, Plot of peak NMDAR currents showing that application of the membrane-permeable PKA activator cpt-cAMP (50 μM) blocked the effect of 8-OH-DPAT (DPAT). Inset, Representative current traces (at time points denoted by #). Calibration: 100 pA, 1 s. N, NMDA. ***B***, Plot of peak NMDAR currents showing that dialysis with the PKA inhibitory peptide PKI[5–24] (40 μM) prevented the 8-OH-DPAT-induced reduction of NMDAR currents. ***C***, Cumulative data (mean ± SEM) showing the percentage reduction of NMDAR currents by 8-OH-DPAT in the absence or presence of agents that affect PKA or PP1. *$p < 0.005$, ANOVA. pI-1, Phosphorylated inhibitor-1 peptide; int; internal. ***D***, Cumulative data (mean ± SEM) showing the percentage modulation of NMDAR currents by 8-OH-DPAT in the absence or presence of the PLC inhibitor U73122 (10 μM), the IP$_3$ receptor antagonist 2APB (15 μM), or the PKC inhibitor calphostin C (1 μM). The number of cells tested in each condition is shown in each bar (***C***, ***D***). ctl, Control.

know whether 5-HT$_{1A}$ receptor activation alters microtubule stability, which could change the dendritic transport of NMDA receptors along microtubules. Biochemical measurements were used to compare the level of free (depolymerized) tubulin in cultured PFC neurons subjected to various drug treatment. As shown in Figure 8*A*, application of 5-HT (40 μM) or 8-OH-DPAT (40 μM) caused a potent increase in free tubulin, similar to the effect of the microtubule-depolymerizing agent colchicine (30 μM), albeit to a smaller extent, indicating that 5-HT$_{1A}$ receptor activation indeed decreases microtubule stability.

We then examined the mechanism underlying the 8-OH-DPAT-induced increase of microtubule depolymerization. As shown in Figure 8*B*, the 5-HT$_{1A}$ receptor antagonist NAN-190 (40 μM) blocked the capability of 8-OH-DPAT to increase free tubulin, indicating the mediation by 5-HT$_{1A}$ receptors. Treatment with the potent microtubule stabilizer taxol (10 μM) almost eliminated free tubulin, and, in the presence of taxol, 8-OH-DPAT failed to elevate the level of depolymerized tubulin. Moreover, the 8-OH-DPAT-induced increase of free tubulin was abolished in the presence of the CaMKII inhibitor KN-93 (10 μM) or MEK inhibitor U0126 (20 μM), suggesting the involvement of CaMKII and ERK signaling pathways in this process. Summarized data are shown in Figure 8*C*.

Activation of 5-HT$_{1A}$ receptors reduces the number of surface NR2B subunits in a microtubule-dependent manner

To morphologically evaluate the changes of NMDAR distribution induced by 5-HT$_{1A}$ receptors, we performed a quantitative surface immunostaining assay in PFC cultures. We transfected neurons with a GFP-tagged NR2B subunit (the GFP tag is placed at the extracellular N terminus of NR2B), which has been shown to exhibit similar properties and localization as endogenous NR2B subunit (Luo et al., 2002). The surface distribution of the recombinant NR2B was assessed by immunostaining with anti-GFP primary antibody followed by rhodamine-conjugated secondary antibody in nonpermeabilized conditions.

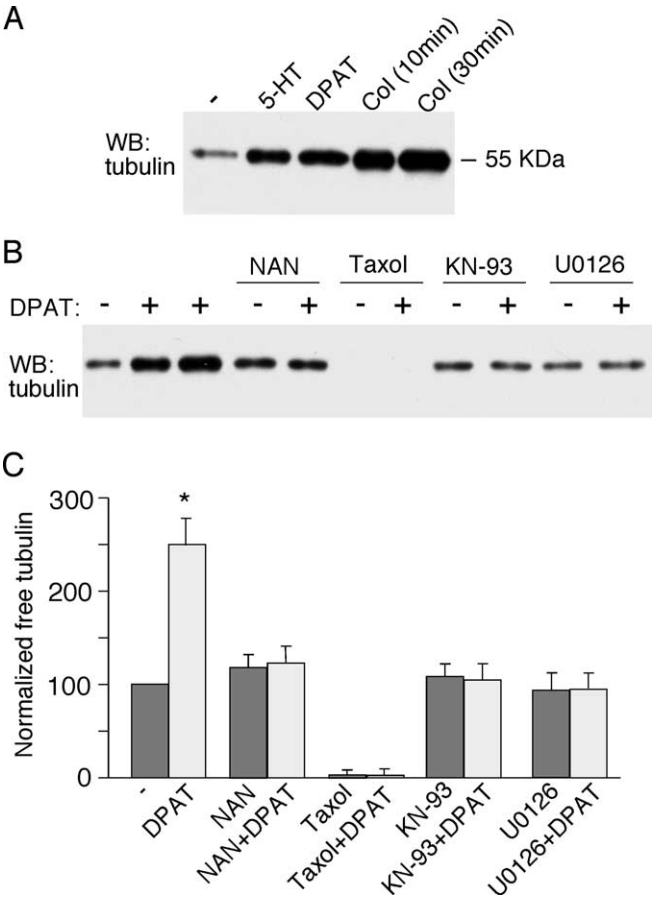

Figure 8. Activation of 5-HT$_{1A}$ receptors induces an increase in free tubulin. ***A***, Western blot (WB) analysis of free tubulin in lysates of cultured PFC neurons treated without (−) or with (+) 5-HT (40 μM, 10 min), 8-OH-DPAT (DPAT; 40 μM, 30 min), or colchicine (Col; 30 μM, 10 or 30 min). ***B***, Western blot analysis of free tubulin in lysates of cultured PFC neurons treated without (−) or with (+) 8-OH-DPAT (40 μM, 30 min; lane 2, 5 min treatment) in the absence or presence of various agents (added 10 min before 8-OH-DPAT treatment), including the 5-HT$_{1A}$ receptor antagonist NAN-190 (NAN; 40 μM), the microtubule stabilizer taxol (10 μM), the CaMKII inhibitor KN-93 (10 μM), and the MEK inhibitor U0126 (20 μM). ***C***, Quantification of free tubulin assay. Free tubulin level was normalized to control (−), based on the intensity of the free tubulin band from Western blot analyses. Each point represents mean ± SEM of four to five independent experiments. *$p < 0.001$, ANOVA.

Punctate red fluorescence was clearly visible on dendritic branches of the GFP-NR2B-transfected cells under control conditions (Fig. 9*A*), whereas in neurons treated with 8-OH-DPAT (40 μM, 5 min), the fluorescent GFP-NR2B surface clusters on dendrites were markedly reduced (Fig. 9*B*). Quantitative analyses (Fig. 9*G*) show that the surface NR2B cluster density on dendrites was significantly decreased (41 ± 3.0 clusters/30 μm in controls vs 24 ± 2.0 clusters/30 μm in 8-OH-DPAT-treated neurons; $p < 0.01$, ANOVA). The average size of surface NR2B clusters on dendrites was also significantly decreased by 8-OH-DPAT (0.30 ± 0.03 μm^2 in controls vs 0.15 ± 0.01 μm^2 in 8-OH-DPAT-treated neurons; $p < 0.01$, ANOVA) (Fig. 9*G*). The fluorescence intensity of surface NR2B clusters (average gray value per pixel) was essentially unchanged (Fig. 9*G*). No staining was observed in either untransfected neurons or neurons transfected with GFP as control. The total amount of NR2B receptor (GFP channel) was not altered by 8-OH-DPAT treatment (data not shown).

We then examined the mechanism underlying the 8-OH-DPAT-induced decrease of surface NR2B. The 5-HT$_{1A}$ receptor antagonist NAN-190 (20 μM) blocked the capability of 8-OH-DPAT to reduce NR2B surface clusters on dendrites [36 ± 2.6 clusters/30 μm in neurons treated with NAN-190 (Fig. 9*C*,*D*) vs 38 ± 1.6 clusters/30 μm in neurons treated with NAN-190 plus 8-OH-DPAT (Fig. 9*G*); $p > 0.1$, ANOVA], indicating the mediation by 5-HT$_{1A}$ receptors. In the presence of the microtubule stabilizer taxol (10 μM), 8-OH-DPAT failed to decrease NR2B surface clusters on dendrites [37 ± 3.4 clusters/30 μm in neurons treated with taxol (Fig. 9*E*,*F*) vs 35 ± 3.9 clusters/30 μm in neurons treated with taxol plus 8-OH-DPAT (Fig. 9*G*); $p > 0.1$, ANOVA]. These results suggest that activation of 5-HT$_{1A}$ receptors reduces the surface NR2B level through a microtubule-dependent mechanism.

Together, these data support a model underlying the serotonergic regulation of NMDA receptor function in PFC pyramidal neurons (Fig. 10). Serotonin, by activating 5-HT$_{1A}$ receptors, causes an inhibition of PKA and subsequent suppression of CaMKII and ERK activity, which results in decreased MAP2 phosphorylation and a subsequent decrease in microtubule stability. Consequently, the KIF17-mediated transport of NR2B-containing vesicles along microtubule in dendrites is disrupted, leading to a significant reduction of the NMDA receptor-mediated currents.

Discussion

In this study, we revealed that activation of 5-HT$_{1A}$ receptors exerted a robust reduction of currents through the NMDA-type glutamate receptor channels, indicating that the NMDA receptor is one of the key targets of 5-HT$_{1A}$ receptors in PFC neurons. Because NMDAR dysfunction has been implicated in mental disorders (Jentsch and Roth, 1999; Tsai and Coyle, 2002), the 5-HT$_{1A}$ interaction with NMDAR channels in PFC could play a significant role in regulating the cognitive and emotional status.

NMDA receptors are found both in the cytoplasm of neurons and at excitatory synapses (Petralia et al., 1994). Emerging evidence has suggested that the NMDA receptor is not a static resident in the plasma membrane and may undergo regulated transport to and from the cell surface and lateral diffusion at synaptic and extrasynaptic sites in the plasma membrane (Wenthold et al., 2003; Collingridge et al., 2004). Several mechanisms have been proposed to be important for stabilizing and/or promoting surface NMDA receptor expression, including the PDZ (PSD-95/Discs large/zona occludens-1) domain-mediated interactions between NR2 subunits and the synaptic scaffolding protein PSD-95 that is regulated by activity-dependent phosphorylation (Roche et al., 2001; Chung et al., 2004; Lin et al., 2004) and tyrosine dephosphorylation of NR1/2A receptors that triggers clathrin-dependent endocytosis (Vissel et al., 2001). Moreover, it has been found that NR2A and NR2B have distinct endocytic motifs and endocytic sorting, with NR2B undergoing more robust endocytosis than NR2A in mature cultures (Lavezzari et al., 2004). However, much remains unknown about the factors regulating the long-range transport of NMDA receptors.

After NR1 and NR2 subunits assemble together to form a functional complex, NMDA receptors overcome the ER retention and are released from the ER. Before being delivered to actin-rich dendritic spines, NMDA receptors are rapidly (4 μm/min) transported along microtubule tracks in dendritic shafts (Washbourne et al., 2002). The dendritic transport of NMDA receptors is mediated by the kinesin motor protein KIF17, which is linked to NR2B-containing vesicles via an mLin complex (Setou et al., 2000). In this study, we found that the 5-HT$_{1A}$ reduction of NMDA receptor currents was mimicked and occluded by the

microtubule-depolymerizing agent nocodazole or colchicine and was blocked by the microtubule-stabilizing compound taxol, but was not affected by the actin-depolymerizing agent latrunculin B or the actin-stabilizing compound phalloidin. Cellular knock-down of the kinesin motor protein KIF17 eliminated the 5-HT$_{1A}$ effect on NMDAR currents. Because 5-HT$_{1A}$ receptors mainly targeted NR2B-containing NMDAR channels (Fig. 2) and KIF17 delivers at least 30% of NR2B in dendrites (Guillaud et al., 2003), our data suggest that the 5-HT$_{1A}$ modulation of NMDA receptors is dependent on the integrity of the microtubule network and involves the transport of NR2B-containing vesicles along microtubules by the molecular motor KIF17.

Microtubules are assembled from heterodimers of α- and β-tubulin. They are highly dynamic structures, undergoing rapid, GTP-dependent transitions between growth and shrinkage states (Cleveland, 1982) and thus have been implicated in regulating nerve growth and dendrite formation (Mitchison and Kirschner, 1988; Vaillant et al., 2002). Two classes of microtubule-binding proteins bind to tubulin polymers and regulate microtubule functions: (1) motor proteins (kinesins and dyneins), which mediate anterograde and retrograde intracellular transport of organelles, vesicles, and proteins along microtubules (Hirokawa, 1998; Goldstein and Yang, 2000); and (2) structural microtubule-binding proteins, such as MAPs, which modulate polymerization and stability of microtubules (Hirokawa, 1994; Mandelkow and Mandelkow, 1995). MAP2, a particular family of MAPs that is highly expressed in neuronal dendrites (Bernhardt and Matus, 1984; Caceres et al., 1984), has been implicated in neurite outgrowth and neuronal plasticity (Sheetz et al., 1998; Sanchez et al., 2000).

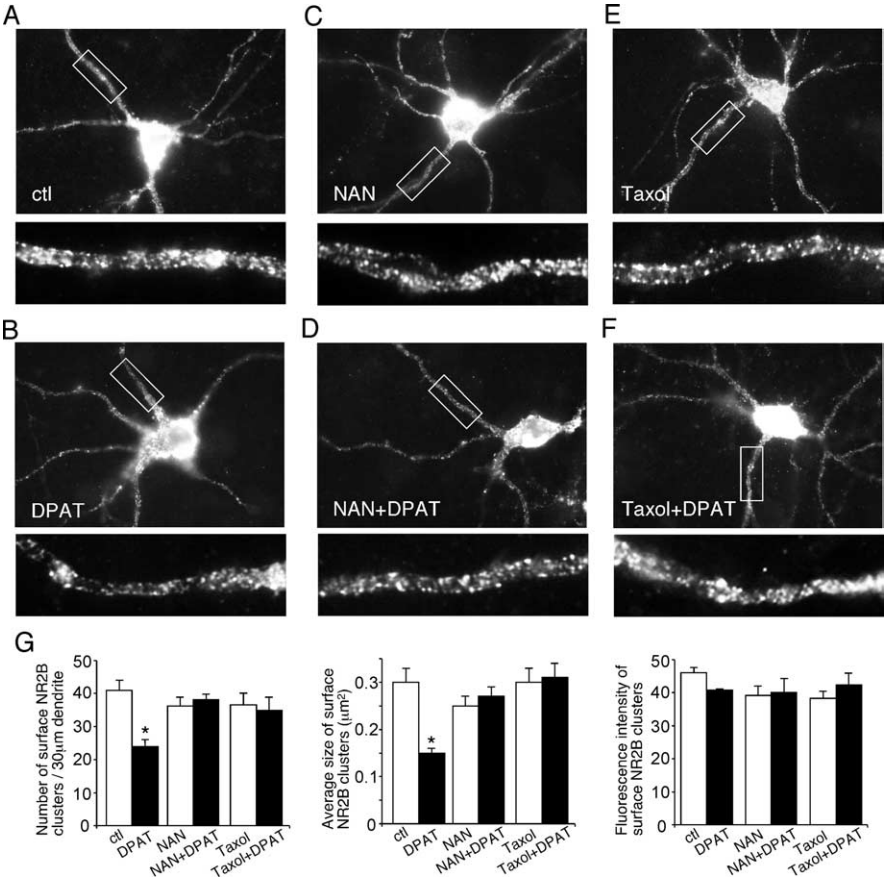

Figure 9. Activation of 5-HT$_{1A}$ receptors decreases the surface NR2B clusters on dendrites. ***A–F***, Immunocytochemical images of surface NR2B in transfected PFC cultures treated without (ctl) or with 8-OH-DPAT (DPAT; 40 μM, 5 min) in the absence or presence of the 5-HT$_{1A}$ receptor antagonist NAN-190 (NAN; 2 μM) or the microtubule stabilizer taxol (10 μM). Enlarged versions of the boxed regions of dendrites are shown beneath each of the images. ***G***, Quantitative analysis of surface NR2B clusters (cluster density, cluster size, and cluster intensity) along dendrites under different treatment. *$p < 0.01$, ANOVA. ctl, Control.

Biochemical studies have identified the dynamic interaction between tubulin and C-terminal domains of NMDAR subunits (van Rossum et al., 1999), but functional studies showing the interaction between microtubules and NMDA receptors are lacking. Our present results suggest that 5-HT$_{1A}$ receptors modulate NMDA receptor currents by interfering with motor protein-mediated vesicle trafficking along microtubules in dendrites. One possible underlying mechanism is that 5-HT$_{1A}$ receptor activation alters the association of MAP2 with microtubules and therefore modifies microtubule stability (Kowalski and Williams, 1993; Dhamodharan and Wadsworth, 1995), leading to the inhibited vesicle trafficking along microtubules in dendrites. Furthermore, because both MAP2 and motor proteins bind to the same C-terminal domain of the tubulin molecule (Hagiwara et al., 1994), MAP2 may interfere with the association of motor proteins with microtubules and therefore inhibits motor-mediated vesicle transport (Heins et al., 1991; Lopez and Sheetz, 1993).

Because MAP2 provides a possible link between 5-HT$_{1A}$ receptor signaling and NMDAR trafficking along microtubules and phosphorylation of MAP2 affects the ability of MAP2 to bind and stabilize microtubules (Brugg and Matus 1991; Itoh et al., 1997), it is likely that 5-HT$_{1A}$ receptor activation changes the phosphorylation state of MAP2, therefore altering microtubule-dependent transport of NMDA receptors. MAP2 proteins are highly phos-

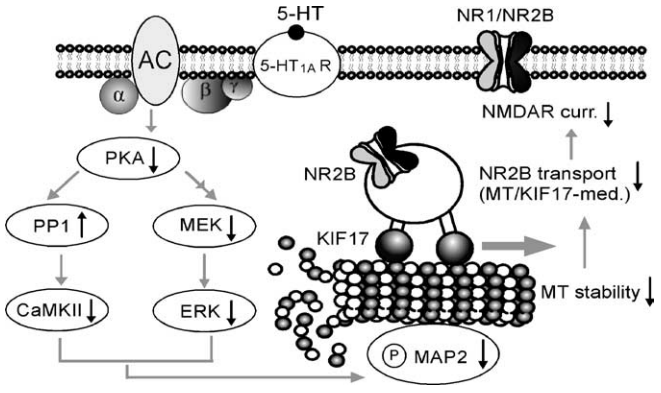

Figure 10. Proposed model showing the mechanisms underlying serotonergic regulation of NMDA receptor function in PFC pyramidal neurons. Activation of 5-HT$_{1A}$ receptors suppresses CaMKII and ERK activity downstream of PKA inhibition, resulting in decreased MAP2 phosphorylation and microtubule (MT) stability and a subsequent disruption of the MT/KIF17-mediated dendritic transport of NR2B-containing vesicles, which leads to a significant reduction of the NMDA receptor-mediated currents. AC, Adenylyl cyclase.

phorylated *in vivo* and are excellent *in vitro* substrates for several protein kinases, including CaMKII, ERKs, PKA, and PKC (Sanchez et al., 2000). Our results show that the 5-HT$_{1A}$ modulation of NMDAR currents was blocked by application of CaMKII inhibitors or suppression of CaMKII expression with a CaMKII siRNA. Application of MEK inhibitors or transfection with the dominant-negative MEK1 also abolished the 5-HT$_{1A}$ effect on NMDAR currents. These data suggest that 5-HT$_{1A}$ receptors signal via CaMKII and ERKs to regulate MAP2 phosphorylation and MAP2–microtubule interactions and hence NMDAR trafficking along microtubules.

The classic pathway for 5-HT$_{1A}$ receptors is to couple to G_i/G_o-proteins to inhibit adenylate cyclase and cAMP formation (Raymond et al., 1999). Our results have shown that the effect of 5-HT$_{1A}$ on NMDAR currents was blocked by stimulating PKA and occluded by inhibiting PKA, indicating that the 5-HT$_{1A}$-mediated reduction of NMDAR currents is dependent on PKA inhibition. Inhibition of PKA could result in the inhibition of the autophosphorylation and autonomous activity of CaMKII through activated PP1 attributable to the decreased phosphorylation of inhibitor-1 (Ingebritsen and Cohen, 1983; Shields et al., 1985; Miller and Kennedy, 1986). Consistent with this, our previous study has shown that 5-HT$_{1A}$ receptor activation reduces CaMKII activity in PFC slices (Cai et al., 2002). Moreover, Inhibition of PKA could result in the inhibition of ERK via the Rap1/B-Raf/MEK signal transduction cascade (Vossler et al., 1997; Roberson et al., 1999).

Our electrophysiological data suggest that 5-HT$_{1A}$ receptor activation, which causes the suppressed CaMKII and ERK activity downstream of the PKA inhibition, leads to the reduction of the number of functional NMDA receptors at the cell membrane via a microtubule-dependent mechanism. Our biochemical measurements have provided direct evidence showing that activation of 5-HT$_{1A}$ receptors indeed decreased microtubule stability, which could lead to the reduction of the delivery of NMDA receptors along microtubules in dendrites. The involvement of CaMKII and ERK in 5-HT$_{1A}$ modulation of NMDA receptors is further confirmed by their role in the regulation of 5-HT$_{1A}$-induced microtubule depolymerization.

To provide more direct evidence on the changes in the distribution of NMDARs in response to 5-HT$_{1A}$ activation, we performed surface labeling of GFP-tagged NR2B subunits (Luo et al., 2002) in transfected PFC neurons. 5-HT$_{1A}$ activation significantly decreased the number and size of surface NR2B clusters on dendritic shafts, an effect blocked by the microtubule stabilizer taxol. These immunocytochemical results further prove that the inhibitory effect of 5-HT$_{1A}$ on NMDAR currents is likely attributable to the reduction of the delivery of NMDA receptors along microtubules in dendrites.

Together, this study provides evidence showing that serotonin, by activating 5-HT$_{1A}$ receptors, suppresses NMDAR function in PFC through a mechanism dependent on microtubule dynamics that is regulated by CaMKII and ERK signaling pathways. Loss of this suppression of excitatory transmission could lead to overactivity of PFC neuronal circuits, as manifested in 5-HT$_{1A}$ knock-out mice, which show the enhanced-anxiety phenotype (Heisler et al., 1998; Ramboz et al., 1998). The 5-HT$_{1A}$ reduction of NMDAR function may also contribute to the 5-HT$_{1A}$ inhibition of long-term potentiation (Sakai and Tanaka, 1993; Edagawa et al., 1998), a synaptic model of learning and memory (Malenka and Nicoll, 1999). Furthermore, compared with typical antipsychotics, the more effectiveness of atypical antipsychotics, which have a significant 5-HT-mediated component of action, in the NMDAR hypofunction model of schizophrenia (Jentsch and Roth, 1999; Meltzer, 1999), may involve the 5-HT–NMDAR interaction revealed in this study. Emerging evidence has suggested that neurons require microtubule-based transport systems to ferry vital cellular cargoes to support their functions, and defects in neuronal transport are linked to the pathogenesis of a number of neuronal diseases (Goldstein, 2003). Thus, the serotonergic regulation of the microtubule/kinesin-based transport system that is responsible for NMDA receptor trafficking provides a potential mechanism underlying the role of 5-HT in controlling emotion and cognition associated with normal mental function and neuropsychiatric disorders.

References

Andrade R (1998) Regulation of membrane excitability in the central nervous system by serotonin receptor subtypes. Ann NY Acad Sci 861:190–203.

Bantick RA, Deakin JF, Grasby PM (2001) The 5-HT1A receptor in schizophrenia: a promising target for novel atypical neuroleptics? J Psychopharmacol 15:37–46.

Bernhardt R, Matus A (1984) Light and electron microscopic studies of the distribution of microtubule-associated protein 2 in rat brain: a difference between dendritic and axonal cytoskeletons. J Comp Neurol 226:203–221.

Brugg B, Matus A (1991) Phosphorylation determines the binding of microtubule-associated protein 2 (MAP2) to microtubules in living cells. J Cell Biol 114:735–743.

Buhot MC (1997) Serotonin receptors in cognitive behaviors. Curr Opin Neurobiol 7:243–254.

Caceres A, Binder LI, Payne MR, Bender P, Rebhun L, Steward O (1984) Differential subcellular localization of tubulin and the microtubule-associated protein MAP2 in brain tissue as revealed by immunocytochemistry with monoclonal hybridoma antibodies. J Neurosci 4:394–410.

Caceres A, Mautino J, Kosik KS (1992) Suppression of MAP2 in cultured cerebellar macroneurons inhibits minor neurite formation. Neuron 9:607–618.

Cai X, Gu Z, Zhong P, Ren Y, Yan Z (2002) Serotonin 5-HT1A receptors regulate AMPA receptor channels through inhibiting CaMKII in prefrontal cortical pyramidal neurons. J Biol Chem 277:36553–36562.

Carli M, Luschi R, Garofalo P, Samanin R (1995) 8-OH-DPAT impairs spatial but not visual learning in a water maze by stimulating 5-HT1A receptors in the hippocampus. Behav Brain Res 67:67–74.

Carroll RC, Zukin RS (2002) NMDA-receptor trafficking and targeting: implications for synaptic transmission and plasticity. Trends Neurosci 25:571–577.

Chen G, Greengard P, Yan Z (2004) Potentiation of NMDA receptor currents by dopamine D1 receptors in prefrontal cortex. Proc Natl Acad Sci USA 101:2596–2600.

Chung HJ, Huang YH, Lau LF, Huganir RL (2004) Regulation of the NMDA receptor complex and trafficking by activity-dependent phosphorylation of the NR2B subunit PDZ ligand. J Neurosci 24:10248–10259.

Cleveland DW (1982) Treadmilling of tubulin and actin. Cell 28:689–691.

Collingridge GL, Isaac JT, Wang YT (2004) Receptor trafficking and synaptic plasticity. Nat Rev Neurosci 5:952–962.

Cull-Candy S, Brickley S, Farrant M (2001) NMDA receptor subunits: diversity, development and disease. Curr Opin Neurobiol 11:327–335.

Davidson RJ, Putnam KM, Larson CL (2000) Dysfunction in the neural circuitry of emotion regulation-a possible prelude to violence. Science 289:591–594.

Dhamodharan R, Wadsworth P (1995) Modulation of microtubule dynamic instability in vivo by brain microtubule associated proteins. J Cell Sci 108:1679–1689.

Dingledine R, Borges K, Bowie D, Traynelis SF (1999) The glutamate receptor ion channels. Pharmacol Rev 51:7–61.

Dubovsky SL, Thomas M (1995) Serotonergic mechanisms and current and future psychiatric practice. J Clin Psychiatry 56 [Suppl 2]:38–48.

Edagawa Y, Saito H, Abe K (1998) 5-HT1A receptor-mediated inhibition of long-term potentiation in rat visual cortex. Eur J Pharmacol 349:221–224.

Feng J, Cai X, Zhao JH, Yan Z (2001) Serotonin receptors modulate GABA$_A$

receptor channels through activation of anchored protein kinase C in prefrontal cortical neurons. J Neurosci 21:6502–6511.
Foulkes JG, Strada SJ, Henderson PJ, Cohen P (1983) A kinetic analysis of the effects of inhibitor-1 and inhibitor-2 on the activity of protein phosphatase-1. Eur J Biochem 132:309–313.
Goldstein LS (2003) Do disorders of movement cause movement disorders and dementia? Neuron 40:415–425.
Goldstein LS, Yang Z (2000) Microtubule-based transport systems in neurons: the roles of kinesins and dyneins. Annu Rev Neurosci 23:39–71.
Grabs D, Slepnev VI, Songyang Z, David C, Lynch M, Cantley LC, De Camilli P (1997) The SH3 domain of amphiphysin binds the proline-rich domain of dynamin at a single site that defines a new SH3 binding consensus sequence. J Biol Chem 272:13419–13425.
Gross C, Hen R (2004) The developmental origins of anxiety. Nat Rev Neurosci 5:545–552.
Gross C, Zhuang X, Stark K, Ramboz S, Oosting R, Kirby L, Santarelli L, Beck S, Hen R (2002) Serotonin1A receptor acts during development to establish normal anxiety-like behaviour in the adult. Nature 416:396–400.
Guillaud L, Setou M, Hirokawa N (2003) KIF17 dynamics and regulation of NR2B trafficking in hippocampal neurons. J Neurosci 23:131–140.
Hagiwara H, Yorifuji H, Sato-Yoshitake R, Hirokawa N (1994) Competition between motor molecules (kinesin and cytoplasmic dynein) and fibrous microtubule-associated proteins in binding to microtubules. J Biol Chem 269:3581–3589.
Heins S, Song YH, Wille H, Mandelkow E, Mandelkow EM (1991) Effect of MAP2, MAP2c, and tau on kinesin-dependent microtubule motility. J Cell Sci 14:121–124.
Heisler LK, Chu HM, Brennan TJ, Danao JA, Bajwa P, Parsons LH, Tecott LH (1998) Elevated anxiety and antidepressant-like responses in serotonin 5-HT1A receptor mutant mice. Proc Natl Acad Sci USA 95:15049–15054.
Hirokawa N (1994) Microtubule organization and dynamics dependent on microtubule-associated proteins. Curr Opin Cell Biol 6:74–81.
Hirokawa N (1998) Kinesin and dynein superfamily proteins and the mechanism of organelle transport. Science 279:519–526.
Ingebritsen TS, Cohen P (1983) Protein phosphatases: properties and role in cellular regulation. Science 221:331–338.
Itoh TJ, Hisanaga S, Hosoi T, Kishimoto T, Hotani H (1997) Phosphorylation states of microtubule-associated protein 2 (MAP2) determine the regulatory role of MAP2 in microtubule dynamics. Biochemistry 36:12574–12582.
Jentsch JD, Roth RH (1999) The neuropsychopharmacology of phencyclidine: from NMDA receptor hypofunction to the dopamine hypothesis of schizophrenia. Neuropsychopharmacology 20:201–225.
Joshi H, Cleveland DW (1989) Differential utilization of beta-tubulin isotopes in differentiated neurites. J Cell Biol 109:663–673.
Kia HK, Miquel MC, Brisorgueil MJ, Daval G, Riad M, El Mestikawy S, Hamon M, Verge D (1996a) Immunocytochemical localization of serotonin1A receptors in the rat central nervous system. J Comp Neurol 365:289–305.
Kia HK, Brisorgueil MJ, Hamon M, Calas A, Verge D (1996b) Ultrastructural localization of 5-hydroxytryptamine1A receptors in the rat brain. J Neurosci Res 46:697–708.
Kim IJ, Drahushuk KM, Kim WY, Gonsiorek EA, Lein P, Andres DA, Higgins D (2004) Extracellular signal-regulated kinases regulate dendritic growth in rat sympathetic neurons. J Neurosci 24:3304–3312.
Kowalski RJ, Williams Jr RC (1993) Microtubule-associated protein 2 alters the dynamic properties of microtubule assembly and disassembly. J Biol Chem 268:9847–9855.
Lavezzari G, McCallum J, Dewey CM, Roche KW (2004) Subunit-specific regulation of NMDA receptor endocytosis. J Neurosci 24:6383–6391.
Lemonde S, Turecki G, Bakish D, Du L, Hrdina PD, Bown CD, Sequeira A, Kushwaha N, Morris SJ, Basak A, Ou XM, Albert PR (2003) Impaired repression at a 5-hydroxytryptamine 1A receptor gene polymorphism associated with major depression and suicide. J Neurosci 23:8788–8799.
Li JH, Wang YH, Wolfe BB, Krueger KE, Corsi L, Stocca G, Vicini S (1998) Developmental changes in localization of NMDA receptor subunits in primary cultures of cortical neurons. Eur J Neurosci 10:1704–1715.
Lin Y, Skeberdis VA, Francesconi A, Bennett MV, Zukin RS (2004) Postsynaptic density protein-95 regulates NMDA channel gating and surface expression. J Neurosci 24:10138–10148.
Lopez LA, Sheetz MP (1993) Steric inhibition of cytoplasmic dynein and kinesin motility by MAP2. Cell Motil Cytoskeleton 24:1–16.
Luo JH, Fu ZY, Losi G, Kim BG, Prybylowski K, Vissel B, Vicini S (2002) Functional expression of distinct NMDA channel subunits tagged with green fluorescent protein in hippocampal neurons in culture. Neuropharmacology 42:306–318.
Malenka RC, Nicoll RA (1999) Long-term potentiation—a decade of progress? Science 285:1870–1874.
Mandelkow E, Mandelkow EM (1995) Microtubules and microtubule-associated proteins. Curr Opin Cell Biol 7:72–81.
Mansour SJ, Matten WT, Hermann AS, Candia JM, Rong S, Fukasawa K, Vande Woude GF, Ahn NG (1994) Transformation of mammalian cells by constitutively active MAP kinase kinase. Science 265:966–970.
Marks B, McMahon HT (1998) Calcium triggers calcineurin-dependent synaptic vesicle recycling in mammalian nerve terminals. Curr Biol 8:740–749.
Martin GR, Eglen RM, Hamblin MW, Hoyer D, Yocca F (1998) The structure and signalling properties of 5-HT receptors: an endless diversity? Trends Pharmacol Sci 19:2–4.
McManus MT, Sharp PA (2002) Gene silencing in mammals by small interfering RNAs. Nat Rev Genet 3:737–747.
Meltzer HY (1999) The role of serotonin in antipsychotic drug action. Neuropsychopharmacology 21:106S–115S.
Miller SG, Kennedy MB (1986) Regulation of brain type II Ca^{2+}/calmodulin-dependent protein kinase by autophosphorylation: a Ca^{2+}-triggered molecular switch. Cell 44:861–870.
Mitchison T, Kirschner M (1988) Cytoskeletal dynamics and nerve growth. Neuron 1:761–772.
Mohn AR, Gainetdinov RR, Caron MG, Koller BH (1999) Mice with reduced NMDA receptor expression display behaviors related to schizophrenia. Cell 98:427–436.
Nong Y, Huang YQ, Ju W, Kalia LV, Ahmadian G, Wang YT, Salter MW (2003) Glycine binding primes NMDA receptor internalization. Nature 422:302–307.
Petralia RS, Yokotani N, Wenthold RJ (1994) Light and electron microscope distribution of the NMDA receptor subunit NMDAR1 in the rat nervous system using a selective anti-peptide antibody. J Neurosci 14:667–696.
Ramboz S, Oosting R, Amara DA, Kung HF, Blier P, Mendelsohn M, Mann JJ, Brunner D, Hen R (1998) Serotonin receptor 1A knockout: an animal model of anxiety-related disorder. Proc Natl Acad Sci USA 95:14476–14481.
Ray LB, Sturgill TW (1987) Rapid stimulation by insulin of a serine/threonine kinase in 3T3–L1 adipocytes that phosphorylates microtubule-associated protein 2 in vitro. Proc Natl Acad Sci USA 84:1502–1506.
Raymond JR, Mukhin YV, Gettys TW, Garnovskaya MN (1999) The recombinant 5-HT1A receptor: G protein coupling and signalling pathways. Br J Pharmacol 127:1751–1764.
Roberson ED, English JD, Adams JP, Selcher JC, Kondratick C, Sweatt JD (1999) The mitogen-activated protein kinase cascade couples PKA and PKC to cAMP response element binding protein phosphorylation in area CA1 of hippocampus. J Neurosci 19:4337–4348.
Roche KW, Standley S, McCallum J, Dune Ly C, Ehlers MD, Wenthold RJ (2001) Molecular determinants of NMDA receptor internalization. Nat Neurosci 4:794–802.
Rosenmund C, Westbrook GL (1993) Calcium-induced actin depolymerization reduces NMDA channel activity. Neuron 10:805–814.
Sakai N, Tanaka C (1993) Inhibitory modulation of long-term potentiation via the 5-HT1A receptor in slices of the rat hippocampal dentate gyrus. Brain Res 613:326–330.
Sanchez C, Diaz-Nido J, Avila J (2000) Phosphorylation of microtubule-associated protein 2 (MAP2) and its relevance for the regulation of the neuronal cytoskeleton function. Prog Neurobiol 61:133–168.
Schreiber R, De Vry J (1993) 5-HT$_{1A}$ receptor ligands in animal models of anxiety, impulsivity and depression: multiple mechanisms of action? Prog Neuropsychopharmacol Biol Psychiatry 17:87–104.
Schulman H (1984) Phosphorylation of microtubule-associated proteins by a Ca^{2+}/calmodulin-dependent protein kinase. J Cell Biol 99:11–19.
Setou M, Nakagawa T, Seog DH, Hirokawa N (2000) Kinesin superfamily motor protein KIF17 and mLin-10 in NMDA receptor-containing vesicle transport. Science 288:1796–1802.
Sheetz MP, Pfister KK, Bulinski JC, Cotman CW (1998) Mechanisms of trafficking in axons and dendrites: implications for development and neurodegeneration. Prog Neurobiol 55:577–594.

Shields SM, Ingebritsen TS, Kelly PT (1985) Identification of protein phosphatase 1 in synaptic junctions: dephosphorylation of endogenous calmodulin-dependent kinase II and synapse-enriched phosphoproteins. J Neurosci 5:3414–3422.

Simpson MD, Lubman DI, Slater P, Deakin JF (1996) Autoradiography with [^{3}H]8-OH-DPAT reveals increases in 5-HT(1A) receptors in ventral prefrontal cortex in schizophrenia. Biol Psychiatry 39:919–928.

Strobel A, Gutknecht L, Rothe C, Reif A, Mossner R, Zeng Y, Brocke B, Lesch KP (2003) Allelic variation in 5-HT1A receptor expression is associated with anxiety- and depression-related personality traits. J Neural Transm 110:1445–1453.

Sumiyoshi T, Stockmeier CA, Overholser JC, Dilley GE, Meltzer HY (1996) Serotonin1A receptors are increased in postmortem prefrontal cortex in schizophrenia. Brain Res 708:209–214.

Tovar KR, Westbrook GL (1999) The incorporation of NMDA receptors with a distinct subunit composition at nascent hippocampal synapses *in vitro*. J Neurosci 19:4180–4188.

Tsai G, Coyle JT (2002) Glutamatergic mechanisms in schizophrenia. Annu Rev Pharmacol Toxicol 42:165–179.

Tyszkiewicz JP, Gu Z, Wang X, Cai X, Yan Z (2004) Group II metabotropic glutamate receptors enhance NMDA receptor currents via a protein kinase C-dependent mechanism in pyramidal neurons of prefrontal cortex. J Physiol (Lond) 554:765–777.

Vaillant AR, Zanassi P, Walsh GS, Aumont A, Alonso A, Miller FD (2002) Signaling mechanisms underlying reversible, activity-dependent dendrite formation. Neuron 34:985–998.

van Rossum D, Kuhse J, Betz H (1999) Dynamic interaction between soluble tubulin and C-terminal domains of *N*-methyl-D-aspartate receptor subunits. J Neurochem 72:962–973.

Vicini S, Wang JF, Li JH, Zhu WJ, Wang YH, Luo JH, Wolfe BB, Grayson DR (1998) Functional and pharmacological differences between recombinant *N*-methyl-D-aspartate receptors. J Neurophysiol 79:555–566.

Vissel B, Krupp JJ, Heinemann SF, Westbrook GL (2001) A use-dependent tyrosine dephosphorylation of NMDA receptors is independent of ion flux. Nat Neurosci 4:587–596.

Vossler MR, Yao H, York RD, Pan MG, Rim CS, Stork PJ (1997) cAMP activates MAP kinase and Elk-1 through a B-Raf- and Rap1-dependent pathway. Cell 89:73–82.

Wang X, Zhong P, Gu Z, Yan Z (2003) Regulation of NMDA receptors by dopamine D_4 signaling in prefrontal cortex. J Neurosci 23:9852–9861.

Washbourne P, Bennett JE, McAllister AK (2002) Rapid recruitment of NMDA receptor transport packets to nascent synapses. Nat Neurosci 5:751–759.

Wenthold RJ, Prybylowski K, Standley S, Sans N, Petralia RS (2003) Trafficking of NMDA receptors. Annu Rev Pharmacol Toxicol 43:335–358.

Williams K (1993) Ifenprodil discriminates subtypes of the *N*-methyl-D-aspartate receptor: selectivity and mechanisms at recombinant heteromeric receptors. Mol Pharmacol 44:851–859.

Yan Z, Hsieh-Wilson L, Feng J, Tomizawa K, Allen PB, Fienberg AA, Nairn AC, Greengard P (1999) Protein phosphatase 1 modulation of neostriatal AMPA channels: regulation by DARPP-32 and spinophilin. Nat Neurosci 2:13–17.

Zhang S, Ehlers MD, Bernhardt JP, Su CT, Huganir RL (1998) Calmodulin mediates calcium-dependent inactivation of *N*-methyl-d-aspartate receptors. Neuron 21:443–453.

Zhong P, Gu Z, Wang X, Jiang H, Feng J, Yan Z (2003) Impaired modulation of GABAergic transmission by muscarinic receptors in a mouse transgenic model of Alzheimer's disease. J Biol Chem 278:26888–26896.